

1 An advanced sequence clustering and designation workflow  
2 reveals the enzootic maintenance of a dominant West Nile  
3 virus subclade in Germany

4 Pauline Dianne Santos<sup>1,†</sup>, Anne Günther<sup>1,†</sup>, Markus Keller<sup>2</sup>, Timo Homeier-Bachmann<sup>3</sup>, Martin H.  
5 Groschup<sup>2,4</sup>, Martin Beer<sup>1</sup>, Dirk Höper<sup>1,†</sup>, Ute Ziegler<sup>2,4,†,\*</sup>

6

7 <sup>1</sup> Friedrich-Loeffler-Institut, Federal Research Institute for Animal Health, Institute of Diagnostic  
8 Virology, 17493 Greifswald-Insel Riems, Germany; [pauline.santos@pei.de](mailto:pauline.santos@pei.de), [anne.guenther@fli.de](mailto:anne.guenther@fli.de),  
9 [dirk.hoeper@fli.de](mailto:dirk.hoeper@fli.de), [martin.beer@fli.de](mailto:martin.beer@fli.de)

10 <sup>2</sup> Friedrich-Loeffler-Institut, Federal Research Institute for Animal Health, Institute of Novel and  
11 Emerging Infectious Diseases, 17493 Greifswald-Insel Riems, Germany; [markus.keller@fli.de](mailto:markus.keller@fli.de),  
12 [martin.groschup@fli.de](mailto:martin.groschup@fli.de), [ute.ziegler@fli.de](mailto:ute.ziegler@fli.de)

13 <sup>3</sup> Friedrich-Loeffler-Institut, Federal Research Institute for Animal Health, Institute of Epidemiology,  
14 17493 Greifswald-Insel Riems, Germany; [timo.homeier@fli.de](mailto:timo.homeier@fli.de)

15 <sup>4</sup> German Centre for Infection Research, partner site Hamburg-Lübeck-Borstel-Riems, 17493  
16 Greifswald-Insel Riems, Germany

17

18 \* Correspondence: [ute.ziegler@fli.de](mailto:ute.ziegler@fli.de); Tel.: +49-38351-71519

19

20 † These authors contributed equally to this work.

21

22

## 23 Abstract

24 West Nile virus (WNV) is the most widespread arthropod-borne (arbo) virus and the primary cause of  
25 arboviral encephalitis globally. Members of WNV species genetically diverged and are classified into  
26 different hierarchical groups below species rank. However, the demarcation criteria for allocating WNV  
27 sequences into these groups remain individual, inconsistent, and the use of names for different levels  
28 of the hierarchical levels is unstructured. In order to have an objective and comprehensible grouping  
29 of WNV sequences, we developed an advanced grouping workflow using the “affinity propagation  
30 clustering”-algorithm and newly included the “agglomerative hierarchical clustering”-algorithm for the  
31 allocation of WNV sequences into different groups below species rank. In addition, we propose to use  
32 a fixed set of terms for the hierarchical naming of WNV below species level and a clear decimal  
33 numbering system to label the determined groups. For validation, we applied the refined workflow to  
34 WNV sequences that have been previously grouped into various lineages, clades, and clusters in other  
35 studies. Although our workflow regrouped some WNV sequences, overall, it generally corresponds  
36 with previous groupings. We employed our novel approach to the sequences from the WNV circulation  
37 in Germany 2020, primarily from WNV-infected birds and horses. Besides two newly defined minor  
38 (sub)clusters comprising only of three sequences each, subcluster 2.5.3.4.3c was the predominant  
39 WNV sequence group detected in Germany from 2018-20. This predominant subcluster was also  
40 associated with at least five human WNV-infections in 2019-20. In summary, our analyses imply that  
41 the genetic diversity of the WNV population in Germany is shaped by enzootic maintenance of the  
42 dominant WNV subcluster accompanied by sporadic incursions of other rare clusters and subclusters.  
43 Moreover, we show that our refined approach for sequence grouping yields meaningful results.  
44 Although we primarily aimed at a more detailed WNV classification, the presented workflow can also  
45 be applied to the objective genotyping of other virus species.

46

## 47 1. Introduction

48 Like other members of the genus *Flavivirus*, West Nile virus (WNV) has become a serious emerging  
49 zoonotic threat in Europe within the last decades (European Centre for Disease Prevention and Control  
50 n.d.; Kuno et al. 1998). The first known case of WNV-infection was reported in Uganda, Africa, in 1937  
51 (Bardos et al. 1959; Smithburn et al. 1940). In the 1960s, the first occurrence of WNV in Europe was  
52 recognized due to neurological disorders in wild and domestic horses in France (Murgue et al. 2001).  
53 Around 30 years later, WNV caused the first severe outbreak of West Nile Fever (WNF) and West Nile  
54 Neuroinvasive Disease (WNND) in humans in Romania (Savage et al. 1999; Tsai et al. 1998). Since then,  
55 WNV has successfully established in various countries. Southern and eastern European countries were  
56 primarily affected by recurring WNV infections in humans, birds, and horses. The highest WNV activity  
57 in Europe was recorded in 2018 (Camp and Nowotny 2020; European Centre for Disease Prevention  
58 and Control 2019). Almost 90% of all locally acquired WNV human infections in Europe, with 166 fatal  
59 cases, were reported in Italy, Greece, and Romania (European Centre for Disease Prevention and  
60 Control 2019). In parallel to this large-scale epidemic in 2018, WNV-RNA positive birds and horses were  
61 confirmed for the first time in Germany (Ziegler et al. 2019). In 2019, a significant increase in WNV  
62 cases in birds and horses as well as the first five autochthonous WNV human infections in Germany  
63 were reported (Robert-Koch-Institut 2020; Ziegler et al. 2020). All prerequisites for endemic WNV  
64 circulation in Germany are fulfilled, including the proven vector competence of local mosquito  
65 populations (Holicki et al. 2020) and the detection of WNV genome-positive mosquito pools (Kampen  
66 et al. 2020; Ziegler et al. 2020).

67 WNV has a diverse host range and is widely distributed. Accordingly, members of this species are  
68 genetically diverse, allowing for the further subgrouping within the species. However, since the  
69 International Committee on Taxonomy of Viruses (ICTV) confines its responsibility to the designation  
70 and demarcation of viruses from realm to species ranks (ICTV 2020; Simmonds et al. 2017), neither a  
71 standard definition of criteria for subgrouping below the species rank nor defined designations for  
72 subgroups and their hierarchical arrangement exist. Therefore, designations for hierarchical ranks

73 (e.g., clade, cluster, sub-type, genotype) are often used inconsistently and interchangeably, leading to  
74 misunderstandings and uncertainties as more and more whole genomes of WNV are generated. Due  
75 to its aforementioned genetic diversity, up to nine lineages have been proposed for the species *West*  
76 *Nile virus* (Fall et al. 2017; Mencattelli et al. 2022; Pachler et al. 2014). The designation “lineage” is  
77 mostly based on monophyletic clustering of partial or whole genome WNV sequences in phylogenetic  
78 analyses (Fall et al. 2017; Perez-Ramirez et al. 2017). However, the lineage classification of WNV strains  
79 remains controversial (Perez-Ramirez et al. 2017). Further subgrouping within the lineages is  
80 conducted to organize viruses into a hierarchical system comprising of various arbitrarily defined and  
81 designated groups. Especially within and between members of WNV lineages 1 and 2 the designations  
82 are used inconsistently. Groups are usually defined based on branching into monophyletic groups from  
83 a common ancestor and members of groups may share common characteristics such as unique and  
84 fixed amino acid (aa) substitutions (Anez et al. 2013; Barzon et al. 2015; Chaintoutis et al. 2019; Davis  
85 et al. 2005; Di Giallonardo et al. 2016; Hadfield et al. 2019; May et al. 2011; McMullen et al. 2013;  
86 Ziegler et al. 2020). Monophyletic groups other than lineages are typically labelled using a letter, region  
87 of origin, or abbreviation of the region of origin (Fall et al. 2017; Kolodziejek et al. 2014; McMullen et  
88 al. 2013; Ravagnan et al. 2015; Zehender et al. 2017; Ziegler et al. 2019; Ziegler et al. 2020).  
89 Noteworthy, nomenclatures based on geographic origin may be misleading. For instance, a WNV  
90 sequence from Italy branched with Eastern European WNV lineage 2 sequences detected in Romania  
91 and Russia (Bakonyi and Haussig 2020; Ravagnan et al. 2015; Sikkema et al. 2020; Ziegler et al. 2020).  
92 Moreover, Ziegler and colleagues (Ziegler et al. 2020) mentioned in the study of the 2018-19 WNV  
93 epidemic in Germany that the label “Eastern German WNV Clade (EGC)”, designated to a group of WNV  
94 sequences from Germany, may not be a suitable designation because “the EGC can have developed in  
95 the wider southeastern and central European hemisphere and may have been translocated only later  
96 to Eastern Germany”. Hence, labels based on geographic origin may not suit the expanding geographic  
97 or undiscovered range of a WNV sequence group.

98 The described situation emphasizes the need for a systematic nomenclature and objective grouping of  
99 WNV sequences into hierarchical groups below the species rank. To subdivide WNV , we further  
100 developed the objective clustering workflow established by Fischer and colleagues (Fischer et al. 2018)  
101 who utilized the affinity propagation clustering (APC) algorithm (Frey and Dueck 2007) as implemented  
102 by Bodenhofer and colleagues (Bodenhofer et al. 2011). However, Fischer and colleagues found  
103 limitations of APC especially for the definition of the best suited number of clusters and therefore  
104 ultimately the definition of groups corresponding with phylogenetic analyses. To solve these issues,  
105 we refined the method to define a suitable number of groups while also incorporating agglomerative  
106 hierarchical clustering (AHC) (Bodenhofer et al. 2011) to address grouping of sequences into multiple  
107 hierarchical levels. In addition, we suggest a decimal numbering system for the hierarchical groups  
108 designated with the proposed unified and consistent labels within the WNV species. Finally, we provide  
109 an update on the WNV situation in birds and horses in Germany 2020 by applying the improved  
110 clustering workflow and our novel generic and consistent nomenclature.

111

## 112 2. Material and Methods

### 113 2.1 WNV screening of birds and horses

114 The nationwide wild bird surveillance program in Germany was established as an instantaneous  
115 reaction to the first Usutu virus (USUV) epizootic in 2011. This monitoring program became reputable  
116 also for the early detection of other zoonotic arboviruses, such as Sindbis virus and WNV. WNV  
117 infection in birds and horses is a notifiable animal disease in Germany if detected by RT-qPCR (real time  
118 quantitative polymerase chain reaction) and/or the identification of WNV-specific IgM in non-  
119 vaccinated horses by ELISA (enzyme-linked immunosorbent assay; i.e. detection of a recent WNV  
120 infection).

121 Samples from birds or horses (e.g. complete animals, organ samples, blood samples, and/or total RNA)  
122 were sent to the national reference laboratory for WNV at the Friedrich-Loeffler-Institut (FLI), Isle of

123 Riems, Germany, by the regional veterinary laboratories of the German federal states, and by members  
124 of the nationwide wild bird surveillance program (for details about the members see (Ziegler et al.  
125 2022)).

## 126 2.2 Ethical statement

127 Bird clinics, veterinarians, wild bird rescue centers and zoos provided bird carcasses for necropsy. In  
128 Germany, no specific permits are required to examine dead birds which have been submitted for  
129 necropsy. Horse clinics and veterinarians from the regional veterinary laboratories provided horse  
130 tissue samples collected in post-mortem examinations by pathological institutions. Residual blood  
131 material was available for one case originating from a WNV-infected bird, collected primarily for  
132 diagnostic purposes and for specific treatment and prognosis.

## 133 2.3 RNA extraction and RT-qPCR

134 Total RNA was extracted from tissue samples (brain, spleen, liver, spinal cord, and/or kidney) and  
135 frozen (-70 °C) coagulated blood samples (cruor). For the first RNA extraction, we applied the RNeasy  
136 Mini Kit (QIAGEN) according to the manufacturer's instructions, followed by screenings for both WNV  
137 lineage 1 and 2 genomes using an RT-qPCR assay (Eiden et al. 2010).

## 138 2.4 Whole-genome sequencing

139 To cover areas with and without previous WNV cases, WNV RNA positive samples from 2020 (Table 1)  
140 were selected for whole-genome sequencing (WGS) primarily based on their geographical location and  
141 C<sub>q</sub> values. In addition, samples from captive birds, wild birds, and horses from similar regions were  
142 included. These selected samples (Table 1) were subjected to a different RNA extraction protocol to  
143 ensure the acquisition of high-quality starting material for WGS. Briefly, each organ homogenate  
144 suspension (250 µl) was lysed in 750 µl TRIzol™ LS Reagent (Invitrogen) or approximately 30 mg tissue  
145 material homogenized in 1 ml TRIzol™ reagent via TissueLyser II (Qiagen) with a 5 mm steel bead for 2  
146 min at 30 Hz. After phase separation, the aqueous phase was processed using the Agencourt®

147 RNAAdvance Tissue kit (Beckman Coulter) and the KingFisher Flex system (Thermo Fisher Scientific)  
148 according to the manufacturer's instructions.

149 WGS of WNV was performed as described (Quick et al. 2017) with some modifications. Briefly, RNA  
150 was reverse transcribed using the SuperScript™ IV First-Strand Synthesis System (Invitrogen) with  
151 random hexamers. The cDNA was subjected to the WNV-specific multiplex PCR described in (Sikkema  
152 et al. 2020). Using two different primer mixes (Table S1) and an AccuPrime™ *Taq* DNA Polymerase Kit  
153 (Invitrogen), two multiplex PCR reactions were performed. Amplicons were purified with 1.8 volume  
154 of Agencourt® AMPure XP beads (Beckman Coulter) and quantified using a NanoDrop™ ND1000  
155 Spectrophotometer (Thermo Fisher Scientific). These two purified and quantified amplicon pools were  
156 combined per sample in equal concentration (125 ng each) and the volume adjusted to 130 µl.  
157 Fragmentation and library preparation steps were performed according to (Wylezich et al. 2018).  
158 Quantified libraries (GeneRead DNA Library L Core Kit; QIAGEN) were sequenced using an Ion Torrent  
159 S5 XL instrument with Ion 530 chips and respective reagents (Thermo Fisher Scientific) in 400 bp mode  
160 according to the manufacturer's recommendations.

161 We verified the PCR-based sequencing using five WNV-positive samples from previous seasons (C1-C5;  
162 Table S2) that had already been sequenced according to the validated approach described in (Wylezich  
163 et al. 2018). Two previously completed libraries of C4 and C5 were enriched for WNV using MyBaits  
164 (Wylezich et al. 2018; Wylezich et al. 2021) but still only yielded partial genome sequences. On the  
165 contrary, the multiplex PCR-based approach generated complete coding sequences of all 5 test  
166 samples, albeit with a truncated 3' end (23-71 nucleotides). The sequences from both approaches were  
167 100% identical for samples C1-C3 and showed a few differences for samples C4 and C5 (Table S2).  
168 These results demonstrated that the multiplex PCR approach is suitable for reliable and sensitive WGS  
169 of WNV, even from samples with low WNV concentration (up to  $C_q$  value 31.5).

170 Sample #26 (ED-I-258/20) had a genome region with a sequencing depth lower than 30, therefore  
171 sequencing results were confirmed with Sanger sequencing. Briefly, cDNA from sample ED-I-258/20  
172 was amplified using additional single-plex PCR assays (primer pairs: WNVUS1\_30\_LEFT and

173 WNVUS1\_30\_RIGHT\_2, WNVUS1\_30\_LEFT\_2 and WNVUS1\_30\_RIGHT). The amplicon was sequenced  
174 with a BigDye Terminator v1.1 Cycle Sequencing kit (Applied Biosystems™, Thermo Fisher Scientific)  
175 on a 3500 Genetic Analyzer Instrument (Applied Biosystems™, Thermo Fisher Scientific).

176 WNV genome sequences obtained in this study were submitted to the European Nucleotide Archive  
177 under the BioProject accession number PRJEB47687.

## 178 2.5 Datasets

179 We validated our workflow using two test datasets consisting of WNV complete coding sequences  
180 previously characterized and classified into different ranks below the species level. “Test dataset 1”  
181 (TD01) consists of 95 WNV whole-genome sequences characterized and classified into different  
182 lineages by Fall and colleagues (Fall et al. 2017). Notably, this study considered WNV clades 1a, 1b, 1c,  
183 4a, and 4b/9 as distinct lineages. “Test dataset 2” (TD02) consists of 150 WNV whole-genome  
184 sequences allocated to three WNV clades and six WNV clade 1a clusters described by May and  
185 colleagues (May et al. 2011). We also combined the sequences from these two test datasets, and a  
186 sequence described as a member of the putative WNV clade 1a cluster 7 (Aguilera-Sepulveda et al.  
187 2021). We referred to these sequences as “test dataset 3” (TD03). Available complete coding  
188 sequences of WNV lineage 2 and their metadata (e.g. sample collection year and country of origin)  
189 were retrieved from GenBank on 10<sup>th</sup> December, 2021. WNV lineage 2 dataset (WL2) consisted of WNV  
190 complete coding sequences from the database and sequences acquired in this study. Accession  
191 numbers of WNV sequences per dataset are summarized in Table S3. We also prepared versions of  
192 these datasets that excluded sequences with  $\geq 10$  ambiguous nucleotides or gaps, and duplicates.

## 193 2.6 *In-silico* analyses

### 194 2.6.1 *Sequence assembly*

195 Genome sequences were assembled from raw data using the Roche/454 genome Sequencer software  
196 suite v3.0 (Roche). Sequencing adapters and PCR primers were trimmed using the Newbler assembler  
197 prior to reference mapping. Initial reference-based mapping against WNV strain 1382/2018/Berlin/Ger



198 (MH986055.1) was done to generate a sample specific consensus sequence. These consensus  
199 sequences were then employed as the reference for a second reference-based mapping per dataset.  
200 The resulting genome sequences were visually inspected using the Geneious Prime® 2021.0.1 software  
201 (Biomatters).

### 202 *2.6.2 WNV genome characterization and phylogenetic analyses*

203 Complete coding sequences from each dataset (TD01, TD02, TD03, WL2) were aligned using the  
204 MUSCLE algorithm (Edgar 2004), and visually inspected using Geneious Prime® 2021.0.1.

### 205 *2.6.3 Maximum likelihood phylogenetic analysis*

206 The best-fitting nucleotide substitution model for each dataset was calculated using jModelTest 2.1.10  
207 (Darriba et al. 2012). Maximum likelihood (ML) inference with the determined best substitution model  
208 and ultrafast bootstrap option (Hoang et al. 2018; Minh et al. 2013) with 100,000 replicates was  
209 performed using IQ-TREE 1.6.8 (Nguyen et al. 2015). ML phylogenetic trees were viewed using FigTree  
210 software (v1.4.4, <http://tree.bio.ed.ac.uk/software/figtree/>).

### 211 *2.6.4 Bayesian phylogenetic analysis*

212 We subjected the dataset consisting of complete genome sequences belonging to the subclade 2.5.3  
213 to the Bayesian Markov Chain Monte Carlo (MCMC) method implemented in the Beast package version  
214 1.10.4 (Drummond and Rambaut 2007; Suchard et al. 2018). We performed regression analyses of the  
215 root-to-tip genetic distance in the resulting ML trees against sampling years using TempEst (Rambaut  
216 et al. 2016). The spatiotemporal dynamics of WNV and the time to most recent common ancestors  
217 (MRCA) were co-estimated using best suited substitution model based on the jModelTesT 2 (Darriba  
218 et al. 2012), optimal molecular clock model (relaxed uncorrelated lognormal) and best demographic  
219 scenario (the Bayesian SkyGrid coalescent model), which will be explained below.

220 The optimal molecular clock model (strict or relaxed uncorrelated log normal) and tree prior (Constant,  
221 Bayesian GMRF Skyride, or Bayesian Skygrid model) were selected based on the marginal likelihood  
222 estimation path sampling and stepping stone sampling methods. The MCMC chain length was run until

223 convergence and sampled every  $10^4$  iterations. Convergence was evaluated by approximating the  
224 effective sampling size (ESS) after a 10% burn-in using the Tracer software version 1.7.1, with ESS  
225 values  $\gg 200$  accepted. The strength of the evidence against  $H_0$  was evaluated according to Kass and  
226 Raftery's (Kass and Raftery 1995) Bayes factor test as follows: Bayes factor (BF) 1-3 – weak, BF 3-20 –  
227 positive, BF 20-150 – Strong, and  $>150$  – very strong (comparison of each parameter summarized in  
228 Table S4).

229 Phylogeographic analysis was performed using a discrete model attributing state characters  
230 represented by the detection of location (country) of each strain and the Bayesian stochastic search  
231 variable (BSSV) algorithm implemented in BEAST v1.10.4 (Suchard et al. 2018). TreeAnnotator v1.10.4  
232 was employed to summarize the maximum clade credibility (MCC) tree after 10% burn-in and Figtree  
233 software v1.4.4 was utilized to visualize the MCC tree. The branches of the trees were color-coded  
234 based on the sample's geographic origin (country).

#### 235 *2.6.5 Affinity propagation clustering (APC)-based workflow for sequence grouping*

236 We analyzed WNV complete coding sequences using a workflow comprising of the APC algorithm and  
237 AHC included in the R package "apcluster" (Bodenhofer et al. 2011) implemented in R v4.1.2 and R  
238 studio (v2021.09.1-372)(R Core Team 2021). The APC algorithm requires a dissimilarity matrix as input  
239 for clustering. For each of the determined clusters, one entity is defined as the "best representative"  
240 or the "cluster exemplar".

241 Using the Sequence Demarcation Tool (SDT; SDT\_Linux64 v1.2) (Muhire et al. 2014), we calculated  
242 pairwise global alignments of the coding sequences and from these alignments used the pairwise  
243 nucleotide identities to calculate a dissimilarity matrix by subtracting the identities from 1.  
244 Subsequently, to increase the robustness and discriminatory power of the APC, these dissimilarities  
245 were squared and converted to negative values according to Fischer and colleagues (Fischer et al.  
246 2018) in order to yield the suitable input data for the APC algorithm.

247 One major problem in clustering is finding the suitable number of clusters to subdivide the dataset  
248 into. To this end, Fischer and colleagues (Fischer et al. 2018) developed the “plateau method” to  
249 calculate the optimum number of clusters. The number of clusters generated by APC is determined by  
250 a parameter called input preference, which by default is set to 0.5. Using the AP clustering algorithm,  
251 the suitable “input preference range” from minimum (pmin) to maximum (pmax) can be calculated.  
252 For the plateau method, the number of clusters (z-value) is repeatedly determined in dependence of  
253 the input preference which is increased in equal steps through the preference range. Usually, with an  
254 increase of the input preference, the number of groups monotonously increases; if a reduction occurs,  
255 this is deemed a disturbance that leads to the termination of the calculations. Fischer and colleagues  
256 defined the best suited number of groups corresponding to the longest plateau that was observed (the  
257 same number of clusters observed consecutively for the highest number of iterations before a  
258 disturbance occurred). While in principle this was suitable, they nevertheless found that it was not  
259 optimal. Since there can be a monotonous increase of the group number without a disturbance  
260 occurring throughout the whole preference range, we tested using the last stable plateau as an  
261 alternative measure for the definition of the group number. The last stable plateau is defined as the  
262 last plateau without disturbance and with at least the set minimal length. For this calculation, we set  
263 the minimum number of iterations that make a plateau to 3. Finally, for the definition of the most  
264 suitable number of groups present in the input data, the following rules were applied: (i) if both the  
265 longest and the last stable plateau resulted in a cluster number higher than the default APC, use the  
266 default; (ii) else, if either or both of the plateaus result in values lower than the default, use the higher  
267 of the values to set the number of groups. This number of groups was then used to calculate the  
268 grouping of the input dataset using the function for AHC from the APC package. The described grouping  
269 was applied for the desired number of sub-grouping levels (ranks below the species level). The R code  
270 used for these calculations is available as supplemental material.

271 In order to test the impact of the number of steps and minimum number of iterations to use as the  
272 cut-off for definition of the last plateau for the determination of the group number, we used the

273 described test datasets. We ran all calculations with all possible combinations of different step  
274 numbers (1,000; 2,000; 5,000; 10,000), minimum plateau lengths (sliding window size 1%, 0.5%, 0.25%,  
275 0.1%, or 0.01% of the step number) and minimum group members to have as input for further sub-  
276 grouping (5; 7; 10). In these tests, we found that the coherence of grouping by the described workflow  
277 and the phylogenetic trees increased with the number of steps and with the reduction of the sliding  
278 window size applied for plateau determination. Notably, with a fixed set of step number and sliding  
279 window size, the impact of the minimal group size increases with the increasing size of the input  
280 dataset. Since our initial tests showed that ambiguities in the sequences and to a lesser extent also  
281 duplicated sequences negatively impact the grouping by the described workflow, we also tested the  
282 different test datasets without duplicate sequences and sequences with  $\geq 10$  ambiguous nucleotides  
283 or gaps. Here, we present results from datasets without sequences having  $\geq 10$  ambiguous nucleotides  
284 or gaps, and only retained one representative for sequences sharing 100% nucleotide identity. Unless  
285 indicated, the used parameter set for the presented results were 10,000 steps, sliding window  
286 proportion resulting in sliding window length 3, and minimum group size 5.

#### 287 *2.6.6 Proposal for WNV group designations*

288 Alongside our new workflow, we here propose to use a generic nomenclature based on a hierarchical  
289 numbering system. This proposal is outlined in Figure 1. Based on the use of designations in the  
290 literature, we propose to designate the levels within the species WNV descending from the species  
291 through lineage, clade, subclade, cluster, and finally subcluster. The subclusters can additionally be  
292 divided further, then carrying a letter as the suffix. The digits representing the different hierarchical  
293 levels are separated by a “.” (compare Figure 1). Here, we examined the grouping in different depths  
294 as indicated for the respective analyses. With the lineage designations we followed the established  
295 lineage numbering; hence, where necessary, lineage designations automatically assigned in the  
296 calculations were replaced by the corresponding established designations.

297        *2.6.7 Combination of the clustering workflow, phylogenetic analyses and*

298                    *geolocation*

299        The assigned hierarchical levels of WNV sequences detected in Germany from 2018-20 were  
300        summarized per new phylogenetic group, collection year, and sample type (wild/captive bird, horse,  
301        mosquitoes, and humans). These were exported as a CSV file into the QGIS Desktop (v3.16.15).

302

303        *3. Results and Discussion*

304        Originally, the goal of this study was to provide an update on the WNV epizootic in Germany in 2020.  
305        However, we encountered significant problems in consistently allocating WNV sequences into  
306        different groups below the species rank, namely:

- 307            1) the lack of objective grouping due to undefined demarcation criteria for the splitting of  
308            sequences into groups, resulting in arbitrarily adjusted groupings, and  
309            2) the missing common group designations below species level within the West Nile Virus species  
310            (and in general) that together with the used nomenclature, which often relies on geographical  
311            terms that due to the spread of the virus no longer fit, result in misleading designations.

312        *3.1 Proposal for a hierarchical WNV nomenclature below the species level*

313        To date, there is no commonly used system in the WNV research community for the definition and  
314        designation of virus groups below the species level. Rather, a substantial number of ways to define  
315        and terms to designate virus groups at different levels of a hierarchical system below the species are  
316        used. These are also different from what is used for other virus species and what is commonly  
317        understood (see Table 2).

318        The designations of the hierarchical levels *inter alia* include the terms “lineage”, “clade”, and “cluster”  
319        (Figure 2). However, the use of the labels to designate different levels of the hierarchical system is  
320        variable. The WNV research community especially uses the term “lineage” to describe a broader

321 hierarchical group consisting of clades and/or subclades, while in other virus species, such as severe  
322 acute respiratory syndrome coronavirus 2 (SARS-CoV-2) and rabies virus (RABV), the term “clade”  
323 defines a broader monophyletic group consisting of subclades and lineages (Campbell et al. 2022;  
324 Rambaut et al. 2020).

325 Moreover, beside the variable use of terms for the designation of hierarchical levels, the criteria used  
326 to define the groups are variable. For instance, Aguilera-Sepulveda et al. (2021); Barzon et al. (2015)  
327 and May et al. (2011) defined clusters found within WNV clade 1a as sequences belonging to a  
328 monophyletic group with a close phylogenetic relationship, with a common ancestor and fixed and  
329 unique amino acid substitutions. In another example, McMullen et al. (2013) defined four clades  
330 (clades 2a – 2d) based on nucleotide identities and monophyletic branching within the phylogenetic  
331 tree. However, the demarcation criteria regarding nucleotide identities or amino acid similarities for  
332 each clade were not clearly defined.

333 Likewise, the labels used to designate the groups are diverse. Often, groups are labelled according to  
334 their first geographic occurrence. Although geographic labels may provide epidemiological information  
335 regarding the origin of the WNV cases, these descriptive labels can cause misrepresentation. For  
336 instance, the geographic range of WNV cases designated to the Lombardy cluster, which consisted of  
337 WNV cases from Lombardy, Italy, as of 2015 (Barzon et al. 2015), is recently expanding. The Lombardy  
338 cluster now also includes WNV sequences from France and Spain (Aguilera-Sepulveda et al. 2022).  
339 Similarly, WNV clade 2d sequences from the European continent were designated according to the  
340 supposed region of the viruses’ origins, like WNV sequences from Russia and Romania that were  
341 designated as the Eastern European lineage 2 WNV (EE, Figure 3) (Cotar et al. 2018; Ravagnan et al.  
342 2015) or WNV sequences from Hungary, Austria, Greece, Serbia, and Italy that were put into the  
343 Central/Southern European lineage 2 WNV (C/SE, Figure 3) (Chaintoutis et al. 2019; Ziegler et al. 2020).

344 Due to the issues outlined above, we set out to design a novel unified system for the hierarchical  
345 organization of WNV (and other viruses) based on (I) an objective definition of subgroups (see  
346 paragraphs 2.6.5 and 3.2), (II) a defined set of names for the different nested hierarchical levels, and

347 (III) a system for group designations that does not rely on geographic or other names that can likely be  
348 subject to change. Although we acknowledge the importance of a universal designation below the  
349 species rank encompassing all virus species, we in part still followed the conventional designation of  
350 WNV sequences below the species rank to prevent any confusion. For the species *West Nile virus*, we  
351 define a term associated with a specific hierarchical level, as summarized in Table 2. We propose to  
352 use the following order of hierarchical groups based on increasing shared genetic identities within the  
353 group: lineages (highest level below the species, as commonly used in the WNV community, level 1),  
354 clade (level 2), subclade (level 3), cluster (level 4), and subcluster (level  $\geq 5$ ). Moreover, we propose to  
355 utilize a generic nomenclature for the defined groups based on a hierarchical numbering system to  
356 designate each group at different hierarchical ranks in a logical and standard manner (Table 2, column  
357 “Suggested Usage”). These generic labels also provide information regarding the hierarchical level  
358 through the number of decimal and/or alphabetical places included (compare Figure 1). Furthermore,  
359 these generic labels can be used continuously even when the group members do not share particular  
360 characteristics, such as geographic origin. Finally, we applied these proposals to WNV sequences from  
361 previously published studies and members of WNV lineage 2 available in the public database to  
362 compare our results with previous classifications.

### 363 *3.2 Application of the developed grouping workflow yields reasonable groups*

364 To address the grouping issues outlined above, we developed a workflow for objective clustering of  
365 sequences into different hierarchical groups below species level. This clustering workflow employs  
366 APC, which is a non-hierarchical mathematical clustering method, with AHC to split the dataset into  
367 groups. This workflow is based on the works of Fischer and colleagues (Fischer et al. 2018), who initially  
368 utilized APC to define objective clusters of RABV sequences. Their group also developed the plateau  
369 method to determine the number of clusters in a given dataset, typically a user-defined parameter  
370 required in clustering programs such as HierBAPS (Cheng et al. 2013), Cluster Picker (Ragonnet-Cronin  
371 et al. 2013), TreeCluster (Balaban et al. 2019), and PhyClip (Han et al. 2019). Furthermore, the workflow  
372 of Fischer and colleagues only requires pairwise identities between all pairs of virus sequences as input.

373 Overall, the method overcomes the need for inputting subjective criteria like number of clusters, the  
374 minimum number of sequences per cluster, or support thresholds for cluster allocation. While Fischer  
375 and colleagues successfully assigned RABV and *Francisella tularensis* isolates into reasonable  
376 objectively defined clusters (Busch et al. 2020; Fischer et al. 2018), the APC results were partly  
377 incongruent with the branching of a RABV phylogenetic tree. This incongruence is potentially caused  
378 by the non-hierarchical clustering properties of the APC algorithm in contrast to the phylogenetic  
379 analysis (Fischer et al. 2018), but could also be caused by an uncertainty of the suitable number of  
380 clusters present in the dataset. Therefore, to improve the workflow, we further developed the  
381 determination of the number of clusters and included AHC to determine the generated clusters. In  
382 order to define multiple hierarchical levels, the method was iteratively applied to subsets of the data  
383 corresponding to the subgroups of the preceding iteration, i.e. higher level in the hierarchy. For  
384 optimization of the parameters, we repetitively analyzed the described test datasets and compared  
385 the results with the grouping as described in the respective studies (Chaintoutis et al. 2019; McMullen  
386 et al. 2013; Ravagnan et al. 2015; Zehender et al. 2017; Ziegler et al. 2020). We found that the minimum  
387 number of sequences per group to be used as input for further subgrouping and the number of  
388 iterations used to define the plateau (the window size) had the major impact on the results. On the  
389 contrary, the overall number of iterations applied to determine the number of clusters only had less  
390 influence. The optimal parameters used for all subsequent analyses were the window size of 3 for the  
391 determination of the longest and last stable plateaus, respectively, and the group size of 5 that was  
392 necessary to further split the group. In order to ensure that the number of iterations did not limit the  
393 quality of the clustering, we used 10,000 iterations throughout.

394 We initially applied the developed workflow with the settings outlined in the previous paragraph to  
395 the test dataset TD03 for the definition of groups within the three proposed levels “lineage”, “clade”,  
396 and “subclade”. Figure 2 shows the result of grouping TD03. According to the used minimum size of a  
397 group to be used as input for further subdivision in the next lower hierarchical level, the grouping  
398 stopped at different levels of the hierarchy. Overall, the objective APC grouping coincides with groups



399 that would be defined when analyzing the tree visually. Most groups we found fit with the traditional  
400 definition of a phylogenetic group being monophyletic. In case of the grouping result for TD03,  
401 however, we received one subclade (1.3.5) that was not intuitively clear at the first glance at the tree  
402 because it was not monophyletic (Figure 2; subclade 1.3.5). This subclade is split in two parts  
403 (interspersed by subclades 1.3.7 and 1.3.8), which are in the graph connected with a dashed line with  
404 arrows pointing inwards. This split is possible since our workflow mainly depends on the nucleotide  
405 identities of pairwise aligned sequences but not on reconstructed hierarchical connections. Looking at  
406 the tree in more detail, it becomes clear that the branch lengths between the three subclade members  
407 are indeed quite short and therefore the grouping makes sense. Hence, we proceeded with the proof-  
408 of-concept for the developed method.

### 409 *3.3 Proof-of-concept for the developed clustering workflow*

410 For the proof-of-concept, we compared our grouping results with published groupings. Using the  
411 abovementioned parameters, we could reproduce the groupings of test datasets TD01 and TD02 as  
412 published (Fall et al. 2017; May et al. 2011) (results not shown). For the combined dataset TD03, we  
413 obtained the grouping shown in Figure 2. Both Fall and colleagues and Rizzoli and colleagues  
414 categorized WNV lineages 1a, 1b, 1c, 4a, and 4b (4/9) as distinct and separate lineages (Fall et al. 2017)  
415 (Rizzoli et al. 2015), while May and colleagues designated the same groups of sequences belonging as  
416 clades 1a, 1b, and 1c which they further subdivided into clusters (May et al. 2011). As can be seen, the  
417 objective grouping of the APC/AHC workflow overall coincides with the previously performed  
418 groupings, albeit at different levels of the hierarchy and hence different labels. At the lineage level,  
419 although lineages 1a, 1b, and 1c (Fall) and 4a and 4b (Fall), respectively, are fused together in one  
420 group each by the APC/AHC workflow, the new defined lineages match those of Fall and colleagues  
421 (Fall et al. 2017). At the next level (clade), our workflow divides the fused lineages into clades, with  
422 lineage 4b (Fall et al. 2017) corresponding to clade 4.3 and lineage 4a (Fall et al. 2017) being subdivided  
423 into clades 4.1 and 4.2. Likewise, lineages 1a, 1b, and 1c (Fall et al. 2017) correspond to clades 1.1 (1c),  
424 1.2 (1b), and 1.3 (1a). At the subclade level of our proposed nomenclature, the clusters that May et al.

425 (2011) defined within lineage 1a match our subclades quite well: the members of the cluster 1a/1 (May  
426 et al. 2011) are comprised within the subclades 1.3.1 and 1.3.2; sequences of cluster 1a/2 are  
427 comprised in subclade 1.3.8; 1a/3 and 1a/4 correspond with subclades 1.3.4 and 1.3.3, respectively;  
428 finally, clusters 1a/5 and 1a/6 are combined into subclade 1.3.5. Notably, subclade 1.3.5 is not a  
429 monophyletic group but in the phylogenetic tree all descend from the same branch and their branch  
430 lengths are very short. Therefore, the co-allocation by APC/AHC is congruent with the minor distances  
431 that are visible in the phylogenetic tree. In summary, although in detail there are a few differences,  
432 overall, the developed objective grouping by APC/AHC yields meaningful and reliable groupings.

433 In addition to the above proof of concept study for the separation of WNV of all lineages into the  
434 different hierarchical levels (lineages, clades, and subclades), we analyzed the WNV lineage 2 complete  
435 coding sequences available in the INSDC databases. As stated above for the first analysis, the grouping  
436 we received overall fit well with what is seen intuitively in the tree. Usually, the observed polyphyletic  
437 interspersed groups, e.g., clades 2.2 and 2.5 in Figure 3, which are in part associated with low ultrafast  
438 bootstrap values in the tree (according to the IQ-Tree documentation, only values above 95 % indicate  
439 trustworthy clades (Minh et al. 2022)) are resolved at the next lower grouping level (in this example at  
440 the subclade level). Here, clade 2.2 (Figure 3) is a polyphyletic group comprising five sequences, which  
441 are at the subclade level separated into subclades 2.2.1 and 2.2.2. This interspersed grouping at the  
442 clade level, which occurs in the APC step based on the pairwise identities, cannot be resolved using  
443 AHC. This incongruency is due to the inherent non-hierarchical characteristics of the APC, as described  
444 by Fischer and colleagues (2018). Similarly, in the deeper grouping of subclade 2.5.3 sequences,  
445 subcluster 2.5.3.4.3a includes WNV sequences that are interspersed in the ML and MCC trees (Figure  
446 4). This subcluster formed a paraphyletic group in both ML and MCC trees, and demonstrated low  
447 ultrafast bootstrap values (<80%) and posterior probability values (<0.6), respectively.

448 The discussed topology in phylogenetic trees depicts the so-called “supercluster”, wherein divergent  
449 subgroups are nested within a more extensive cluster structure (Han et al. 2019). Therefore, in  
450 combination with phylogenetic trees our grouping workflow can also provide insights regarding the

451 source-sink ecological dynamics of WNV lineage 2 in Europe. This dynamic has been previously  
452 discussed in the phylogeographic and phylodynamic analyses of Zehender et al. (2017) and Ziegler et  
453 al. (2020). Specifically, cluster 2.5.3.4 may represent the putative source of the WNV population that  
454 gives rise to its subgroups, reflecting the trajectory and divergence of variants (Han et al. 2019). In  
455 parallel, members of cluster 2.5.3.4 were detected in locations described as “radiation centers or  
456 sources” of WNV lineage 2 migration in Europe (e.g., Hungary and Austria). Furthermore, members of  
457 other WNV clusters were detected in areas described as “receiving areas or sinks” of WNV migration,  
458 such as Greece (cluster 2.5.3.3).

459 To further verify the workflow, we compared our grouping with previously published results of  
460 McMullen et al. (2013), Ravagnan et al. (2015), Zehender et al. (2017), Chaintoutis et al. (2019) and  
461 Ziegler et al. (2020). Noteworthy, all studies that were available for comparison only included partial  
462 sets of the sequences that we included here. The comparison of the results of the objective APC/AHC  
463 grouping and the clades defined by McMullen (McMullen et al. 2013) shows that there are two main  
464 differences between both: (i) McMullen’s clade 2b is disrupted into clades 2.3 and 2.4 in our grouping;  
465 this is likely caused by the inclusion of the 2020 sequence from Namibia (MW383507), which forms  
466 clade 2.4 together with the 1958 South African sequence (HM147822) that was included in McMullen’s  
467 clade 2b; (ii) the sequences comprised in McMullen’s clade 2d were now put into clade 2.5, except for  
468 1990 Senegal (DQ318019) and 1937 Uganda (NC\_001563) that form clade 2.2 together with one 1988  
469 sequence from Madagascar (HM147823). These two deviations show the expectable effect of addition  
470 of sequences on tree topology and sequence grouping. The comparison between the groupings of  
471 Ravagnan and colleagues (Ravagnan et al. 2015) and ours shows that the virus group designated  
472 “Eastern European lineage 2 WNV” (labelled EE in Figure 3) coincides with our subclade 2.5.4 and those  
473 of the “Central/Southern European lineage 2 WNV” (labelled C/SE in Figure 3) are all grouped into  
474 subclade 2.5.3. In the studies of Zehender et al. (2017), Chaintoutis et al. (2019) and Ziegler et al.  
475 (2020), viruses belonging to Ravagnan’s C/SE lineage 2 WNV (Ravagnan et al. 2015) were subdivided  
476 into two groups. These were labelled clade A (Zehender) or Central and Eastern European clade (CEC;

477 Ziegler; Chaintoutis) and clade B (Zehender) or Southeastern European clade (SEEC; Ziegler;  
478 Chaintoutis), respectively. Using our APC/AHC workflow, they are grouped together in subclade 2.5.3.  
479 At the next hierarchical level (cluster), with a single exception (LR743454, Germany 2019, cluster  
480 2.5.3.2), clade A/CEC is completely comprised within cluster 2.5.3.4. Likewise, clade B / SEEC is fully  
481 comprised in cluster 2.5.3.3, except for the two sequences from Hungary 2014 (KT359349) and Serbia  
482 2010 (KC496016). Interestingly, cluster 2.5.3.1 comprises only a single WNV sequence from Austria  
483 (KP780840) that has not been included in previous phylogenetic studies (Chaintoutis et al. 2019; Ziegler  
484 et al. 2020) since it was considered an outlier based on its temporal signal relative to other WNV  
485 subclade 2.5.3 sequences. This sequence also showed the lowest pairwise nucleotide identities among  
486 members of subclade 2.5.3. Noteworthy, Ziegler and colleagues highlighted that LR743454 formed its  
487 own distinct subclade within the CEC. In our analysis, this sequence received two companions,  
488 altogether forming cluster 2.5.3.2.

489 Taken together, the presented comparisons between published studies and the grouping obtained by  
490 application of the newly developed APC/AHC workflow show that our objective workflow reliably puts  
491 sequences into meaningful groups.

#### 492 *3.4 WNV circulation in Germany extended in space and species*

493 In 2020, we detected 65 birds (captive = 33 and wild = 32) and 22 horses that tested positive for WNV  
494 in Germany (diagnosed between July 14 and October 20 and two retrospective cases from 2021). All  
495 but one WNV-positive bird succumbed to infection (Table 1; #44). The number of notifiable cases of  
496 WNV in birds and horses in 2020 is similar to the previous year, particularly in regions with the highest  
497 WNV activity i.e., Berlin, Saxony, and Saxony-Anhalt (Figure 5) (Ziegler et al. 2020). However, we  
498 observed an increasing number of WNV-cases in Brandenburg, Thuringia, and Lower Saxony. All WNV-  
499 positive birds and horses detected in 2020 were found in federal states which also reported WNV cases  
500 in 2018 and 2019 (Figures 5 and S1) except for a new WNV-case detected in Lower Saxony. Notably,  
501 all 22 probable autochthonous human WNV cases in 2020 occurred in these federal states (Berlin = 7;  
502 Saxony = 11; Saxony Anhalt = 4) (European Centre for Disease Prevention and Control 2020; Frank et

503 al. 2022; Pietsch et al. 2020). Therefore, this kind of WNV surveillance in both wildlife and captive  
504 animals could provide an early warning for autochthonous WNV-infection in humans in Germany.  
505 Hence, reports of WNV infection in birds and horses in an area must be provided promptly (e.g.,  
506 updates of FLI websites) to advise the medical community and the public regarding a potential risk of  
507 WNV-infection in specific regions in Germany, as well as the risks in blood transfusion and organ  
508 transplantation safety. Although vaccines against WNV disease in humans are still under development  
509 (Ulbert 2019), clinicians must be aware of the potential presence of WNV circulation in the local region  
510 to reach a correct diagnosis since WNV diagnostics is not routinely performed in Germany (Schneider  
511 et al. 2021).

512 Here we report the first case of a WNV-infection in Lower Saxony, where a horse with WNV-specific  
513 IgM antibodies was detected in the Helmstedt district, and the first reported cases of WNV-infected  
514 birds in Thuringia, particularly in the districts of Erfurt and Gera (Figures 5 and S1). We also reported  
515 the first cases of WNV-infection in three districts in Brandenburg (i.e., Teltow-Fläming, Barnim and  
516 Dahme-Spreewald) and in one district in Saxony-Anhalt (Börde) (Figure S1). Areas with reported WNV-  
517 infection match with areas with high average temperatures ( $>20^{\circ}\text{C}$ ), lower average precipitation ( $\leq 250$   
518 mm), and lower average climatic water balance ( $-150 - 50$  mm) in summer 2020 (Figure S2) (Deutscher  
519 Wetterdienst 2020). Higher average temperatures over several days may increase the risks of WNV  
520 transmission through mosquito vectors (Holicki et al. 2020). The higher average temperatures in these  
521 areas probably caused the epizootic emergence of WNV by shortening the extrinsic incubation period  
522 (EIP) in local mosquito populations. Furthermore, WNV activity is more likely to increase during  
523 drought than during rainy periods (Paull et al. 2017). It is also possible that the declining water sources  
524 force the avian reservoir hosts to aggregate, increasing the probability of contact between birds and  
525 mosquitoes and WNV transmission (Paull et al. 2017). However, we did not detect the re-emergence  
526 of WNV in Hamburg, and in two districts in Brandenburg (Ostprignitz-Ruppin and Havelland) in 2020,  
527 despite the observed higher average temperatures ( $>20^{\circ}\text{C}$ ) and lower average precipitations (126-200  
528 mm) in summer 2020.

529 We also detected WNV infections in 21 different bird species from six taxonomic orders (Table 3). The  
530 majority of WNV-infected avian species are classified as birds of prey (order *Accipitriformes*, 29%),  
531 followed by songbirds (order *Passeriformes*, 26%), captive flamingos (order *Phoenicopteriformes*, 23%)  
532 and owls (order *Strigiformes*, 17%). Most of the WNV-infected bird species in 2020 were also reported  
533 in an earlier study (Ziegler et al. 2020), except for the alpine chough (*Pyrrhocorax graculus*), Bohemian  
534 waxwing (*Bombycilla garrulus*), and golden eagle (*Aquila chrysaetos*). However, all three species  
535 belong to taxonomic orders that were already described before to be repeatedly affected by WNV  
536 (*Passeriformes* and *Accipitriformes*) (Michel et al. 2018; Michel et al. 2019). Notably, the golden eagle  
537 from Brandenburg (#44) is the only reported case in 2020 that recovered from WNV-infection (Table  
538 1).

### 539 3.5 Update on the WNV situation in Germany, 2020

540 After we had validated the workflow, we analyzed the ongoing WNV epizootic in Germany using this  
541 tool. The result of grouping sequences that belong to subclade 2.5.3, to which all viruses circulating in  
542 Germany until 2020 belong, is shown in Figure 4. As can be seen, subclade 2.5.3 can be further  
543 subdivided into the four clusters 2.5.3.1, 2.5.3.2, 2.5.3.3, and 2.5.3.4. Interestingly, cluster 2.5.3.1 only  
544 comprises the beforementioned Austrian sequence KP780840 that was previously deemed an outlier  
545 and therefore disregarded in previous analyses. Cluster 2.5.3.2, which can due to the group size  
546 restriction also not be further subdivided, consists of three German sequences (LR743454 from 2019  
547 and #32 and #37 from 2020), also mentioned above. On the contrary, clusters 2.5.3.3 and 2.5.3.4 can  
548 be further subdivided into multiple subclusters each. Although to a large extent the detected  
549 subclusters comprise sequences from individual countries, they are clearly not geographically  
550 homogenous, highlighting the problem of geographic criteria for the designation of phylogenetic  
551 groups. For instance, subcluster 2.5.3.4.3b mainly comprises sequences from Italy but also 2 from  
552 France and 1 sequence of a case imported to Germany (MH910045). Likewise, subcluster 2.5.3.4.3c,  
553 into which the majority of WNV sequences from Germany were grouped, also comprises sequences  
554 from Slovakia (n=2), Austria (n=5), and the Czech Republic (n=2).

555 As summarized in Figures 6 and 7, sequences from WNV circulating in Germany from 2018-20 were  
556 allocated to cluster 2.5.3.2 and subclusters 2.5.3.4.3a and 2.5.3.4.3c, respectively. A sequence of  
557 cluster 2.5.3.2 was first detected in 2019 (LR743454) and previously formed an outlier (Ziegler 2020)  
558 but now two additional viruses of this cluster were detected (ED-I-228-20 - #32, ED-I-210-20 - #37)  
559 (Figure 6). The MRCA of WNV in cluster 2.5.3.2 (see Figure 4) was estimated to have existed around  
560 2018 (95% highest posterior density or 95% HPD: 2017- 2019; Bayesian posterior probabilities or pp:  
561 100%). Unlike viruses of cluster 2.5.3.2, viruses of subcluster 2.5.3.4.3a were only detected in 2018  
562 (ED-I-127-18 – C5) and 2019 (LR743431, LR743448), but not in 2020 (Figure 6). Given the available  
563 WNV genome sequences, we cannot confirm whether these minor genotypes (cluster 2.5.3.2 and  
564 subcluster 2.5.3.4.3a) have successfully overwintered or been introduced to Germany in separate  
565 events. Furthermore, we may have missed these minor WNV clusters and subclusters as we could not  
566 sequence all WNV-positive cases from 2018-20 (Table 1; #45). For instance, most horse samples are  
567 serologically WNV IgM positive but WNV-RNA negative, preventing the successful sequencing of WNV  
568 genomes. Moreover, organ materials from small passerines were often depleted after necessary  
569 routine diagnostics at the regional veterinary laboratories for other relevant avian viruses or after  
570 confirmatory diagnostics at the national reference laboratory at the FLI. In some cases, simply the  
571 sample quality and/or quantity prevents from generating the genome sequences, despite the use of  
572 the WNV multiplex-PCR-based HTS approach (Sikkema et al. 2020).

573 Beside the above mentioned two minor groups, the vast majority of WNV circulating in Germany were  
574 allocated to subcluster 2.5.3.4.3c, which comprises all sequences previously allocated to the EGC plus  
575 additional sequences, inter alia two previously defined minor subclades comprising sequences  
576 LR743422 and LR743437/LR743434 (Ziegler et al. 2020). The EGC, which was the dominant genotype  
577 that circulated in Germany from 2018-19, was characterized by a unique non-synonymous mutation  
578 (Lys<sub>2114</sub>Arg) located within the NS3 encoding genome region (noteworthy, LR743444 and LR743425  
579 were previously designated into the EGC but do not harbor this mutation). This mutation no longer is  
580 a marker of the respective group (subcluster 2.5.3.4.3c) which also comprises sequences without that

581 specific mutation. Overall, the grouping we now observed (one major subclade and two minor  
582 (sub)clusters agrees with our previous WNV report, wherein we detected six distinct “subclades”  
583 circulating in Germany in 2018 and 2019 (Ziegler et al. 2020).

584 We estimated that the MRCA of the monophyletic branch consisting of subcluster 2.5.3.4.3c sequences  
585 existed around 2010 (95% HPD: 2008–2011; pp: 100%). Despite the fact that the vast majority of the  
586 2.5.3.4.3c sequences are from Germany, it appears highly unlikely that the ancestors of that subcluster  
587 evolved in Germany, as confirmed WNV-positive cases in Germany were only detected from 2018  
588 onwards by the extensive arbovirus monitoring performed in the country since 2011 (Michel et al.  
589 2019; Ziegler et al. 2022). Rather, given that (i) the estimated MRCA of the EGC coincided with large  
590 reported outbreaks in eastern and southeastern Europe (Aberle et al. 2018; Jungbauer et al. 2015;  
591 Kolodziejek et al. 2015; Kolodziejek et al. 2018; Rudolf et al. 2014; Sedlak et al. 2014; Vlckova et al.  
592 2015) and (ii) WNV complete genomes are not available from neighboring countries, we cannot  
593 determine where this subcluster diverged. Therefore, we hypothesize that members of the EGC were  
594 more likely introduced to Germany from neighboring countries in separate events and in a later time  
595 than its estimated MRCA.

596 While we detected subcluster 2.5.3.4.3c all over the WNV affected regions in Germany from 2018 until  
597 2020, making it the dominating subcluster, viruses of (sub)cluster 2.5.3.2 and 2.5.3.4.3a were both in  
598 time and space restricted and of minor impact for the ongoing epizootic (Figures 6 and 7). Like with  
599 the sporadic occurrence of the aforementioned two (sub)clusters, there are also regions within  
600 Germany where WNV occurrence is only sporadic (regardless of the virus’ phylogenetic group).  
601 Namely, we detected WNV infected wild birds in Rostock, Mecklenburg-Western Pomerania in 2018  
602 (n=1) and in Hamburg (n=1), Havelland, Brandenburg (n=1) in 2019. However, in these areas in the  
603 succeeding years, WNV activity was not reported.

604 As in the preceding years, in 2020, except for two cases in which viruses of cluster 2.5.3.2 were  
605 detected, all other viruses were grouped into subcluster 2.5.3.4.3c, and in the same cities and districts  
606 as before (Figure 7). In addition, viruses of subcluster 2.5.3.4.3c were detected in three districts in



607 Thuringia. These observations suggest that viruses of subcluster 2.5.3.4.3c successfully established in  
608 local avian and mosquito populations in the affected regions, namely in Berlin, Saxony (particularly  
609 within Leipzig and neighboring areas) and Saxony-Anhalt, which led to the endemic circulation of WNV  
610 in these areas in 2020. We also observed the continuous geographic expansion of WNV belonging to  
611 subcluster 2.5.3.4.3c from 2018 to 2020; however, only time will tell whether members of this  
612 subcluster successfully overwinter and establish themselves in these newly affected areas. In 2021,  
613 however, WNV cases in birds and horses were predominantly reported in Berlin, with a few additional  
614 WNV-cases reported in Saxony, Saxony-Anhalt, and Brandenburg (FLI report).

615 WNV sequences within subcluster 2.5.3.4.3c from Germany were acquired from mosquito pools (n=2),  
616 horses (n=2) and different bird species (n=78) belonging to seven taxonomic orders. Complete coding  
617 sequences from five human WNV cases reported from 2019 (n=1) to 2020 (n=4) were also allocated  
618 into WNV subcluster 2.5.3.4.3c (Figure 6). We excluded a few human WNV cases where either only a  
619 partial genome sequence (n=2) (Pietsch et al. 2020; Ziegler et al. 2020) or no sequence information at  
620 all (n=3) (Ziegler et al. 2020) was available. These WNV cases did not meet the required criteria for the  
621 APC/AHC grouping, i.e., WNV complete coding sequences with <10 nucleotide gaps or ambiguities. As  
622 expected, the available partial WNV genome sequences of the two human cases (MN794936,  
623 MW142225) had the highest sequence identities with members of the subcluster 2.5.3.4.3c. In  
624 addition, recently published complete coding sequences (MZ964751.1, MZ964752.1, MZ964753.1)  
625 from three human WNV cases reported in 2021 (Schneider et al. 2021) have the highest sequence  
626 identities with members of subcluster 2.5.3.4.3c. Therefore, as of writing, only members of subcluster  
627 2.5.3.4.3c have been reported to cause WNV infection in humans in Germany. Members of subcluster  
628 2.5.3.4.3a, likewise detected in Germany, have previously been reported to cause human WNV-  
629 infection in other countries, i.e. Austria (Kolodziejek et al. 2015; Kolodziejek et al. 2018). The higher  
630 spread and frequency of subcluster 2.5.3.4.3c in Germany are the likely cause for it being the sole  
631 subcluster so far associated with human WNV cases reported in Germany.

632 Here, we also obtained the complete coding sequence of WNV detected in a horse from 2018 (C5),  
633 grouping in subcluster 2.5.3.4.3a (Figures 4 and 7). Viruses of subcluster 2.5.3.4.3a are found  
634 widespread across Europe over a long period of time, e.g., in Italy (2011), Austria (2015-2016), the  
635 Czech Republic (2013), Slovakia (2013), Slovenia (2018), Germany (2018-2019), and the Netherlands  
636 (2020) (Figure 4). Noteworthy, we did not find any member of this subcluster among the sequenced  
637 WNV cases in 2020. Still, we cannot directly conclude that its absence in 2020 was due to a failed  
638 establishment in Germany since we were not successful in generating sequences from all 65 WNV PCR-  
639 positive birds from the 2020 season. The MRCA of WNV MW036634, detected in a *Culex* mosquito  
640 pool collected in Utrecht, the Netherlands, in 2020 (Sikkema et al. 2020) and LR743448 (collected in  
641 Cottbus, Brandenburg, Germany in 2019) was predicted to exist around 2013 (HPD 95%: 2011-2015  
642 and pp: 35%) (Figure 4). However, these WNV cases from Cottbus and Utrecht were detected >600 km  
643 apart within a short period. Given the large distance between Utrecht and Cottbus together with the  
644 ubiquitous distribution of subcluster 2.5.3.4.3a in Europe, we suspect that these two WNV cases might  
645 be independent of each other, although they are the closest known relatives. Due to the greater  
646 distances between the Netherlands and those regions of Europe where related WNV were previously  
647 detected, we hypothesize that different modes of WNV dispersal other than bird migration may have  
648 played a role to the WNV introduction in the Netherlands. For instance, the translocation of WNV-  
649 infected mosquitoes inside vehicles (planes, ships, automobiles) may have occurred as described for  
650 different mosquito species (Bakran-Lebl et al. 2021; Brown et al. 2012; Eritja et al. 2017; Ronca et al.  
651 2021).

652

## 653 Conclusions

654 Here, we introduced a structured and unbiased clustering workflow to systematically allocate WNV  
655 complete coding sequences to at least six hierarchical groups below the species level: **lineages**, **clades**,  
656 **subclades**, **clusters**, and **subclusters**. In addition, we propose a generic hierarchical decimal numbering  
657 system designating each group below species rank. We successfully applied the method to allocate

658 WNVs into groups below the species level and this workflow can also be applied to classify other virus  
659 species into hierarchical subgroups. Our workflow only requires a matrix of pairwise sequence  
660 identities as input. Essential parameters (e.g. number of clusters, threshold, etc.) are entirely decided  
661 by the mathematical algorithm, thus removing subjective input from users. Furthermore, the results  
662 of our workflow can be combined with different analyses, such as the classical phylogenetic ML tree  
663 and the time-scaled MCC tree.

664 Our analyses revealed that subcluster 2.5.3.4.3c was the predominant WNV subcluster circulating in  
665 Germany from 2018-20, accompanied by co-circulating minor WNV (sub)clusters. This finding indicates  
666 that the WNV genetic diversity in Germany is primarily influenced by the successful establishment,  
667 enzootic maintenance and expansion of subcluster 2.5.3.4.3c, possibly supplemented with continuous  
668 incursion and potential overwintering of WNV of other (sub)clusters. These other (sub)clusters  
669 detected in Germany overlapped in space and time with the dominant subcluster 2.5.3.4.3c. The minor  
670 groups were found in both wild and captive birds, as well as in horses. Therefore, to obtain the full  
671 picture of WNV circulation, it will be necessary to obtain whole-genome sequences from all WNV-cases  
672 whenever possible, to ensure that also minorities are found.

673 Since all human WNV cases in 2020 occurred in WNV hot spot areas, our study affirmed the importance  
674 of birds and horses as sentinels for human WNV-infections. Thus, information dissemination regarding  
675 WNV-infections should be conducted among healthcare and veterinary workers and the greater public.  
676 Furthermore, we recommend that horses located in these WNV hotspot areas and nearby regions be  
677 vaccinated against WNV according to the recommendations of the Standing Committee on Vaccination  
678 for Veterinary Medicine in Germany (StIKo Vet).

679

## 680 [Acknowledgements](#)

681 We are grateful to Patrick Zitzow, Cornelia Steffen, Katja Wittig, and Katrin Schwabe for excellent  
682 technical assistance. We are indebted to Dr. Susanne Fischer for the significant input regarding affinity

683 propagation clustering. We thank Sabine Bock (Berlin-Brandenburg State Laboratory, Frankfurt  
684 (Oder)), Kerstin Albrecht (State Institute for Consumer Protection of Saxony-Anhalt, Department of  
685 Veterinary Medicine, Stendal), Andrea Konrath (Saxon State Laboratory of Health and Veterinary  
686 Affairs, Leipzig), Aemero Muluneh (Saxon State Laboratory of Health and Veterinary Affairs, Dresden),  
687 Timo Siempelkamp (Thuringia Office for Consumer Protection, Bad Langensalza), Michael Sieg  
688 (Institute of Virology, Faculty of Veterinary Medicine, Leipzig University, Leipzig), Claudia Szentiks  
689 (Leibniz Institute for Zoo and Wildlife Research, Berlin), Dominik Fischer (Clinic for Birds, Reptiles,  
690 Amphibians and Fish, Justus Liebig University Giessen, Giessen), Claudia Sauerwald (Landesbetrieb  
691 Hessisches Landeslabor, Veterinary Virology and Molecular Biology, Gießen) and the other colleagues  
692 of the veterinary authorities and veterinary laboratories of the federal states for the supply of the  
693 samples and we are very grateful for the continuous support. Furthermore, we thank the staff of the  
694 different bird clinics, rehabilitation centers, zoological gardens and “Tierparks” of Germany as partners  
695 in the nation-wide wild bird surveillance network for zoonotic arthropod-borne viruses, which  
696 collected and sent samples for the present study. Furthermore, we want to thank Patrick Wysocki and  
697 Daike Lehnau (Institute of Epidemiology, FLI, Greifswald-Insel Riems) for their help by producing the  
698 epidemiological datasets and Jacqueline King (Institute of Diagnostic Virology, FLI, Greifswald-Insel  
699 Riems) for proofreading the manuscript.

700 This work was funded by European Union’s Horizon 2020 research and innovation program under the  
701 Marie Skłodowska-Curie Actions grant agreement no. 721367 (HONOURS) and in part by the EU  
702 Horizon 2020 program grant agreement no. 874735 (VEO) and by the German Federal Ministry of Food  
703 and Agriculture (BMEL) through the Federal Office for Agriculture and Food (BLE), grant number  
704 2819113919 (CuliFo2) as well as by the German Center for Infection Research (DZIF) under project  
705 number TTU 01.804 (WBA-Zoo), and by the Federal Ministry of Education and Research within the  
706 research consortium “ZooBoCo” (Grant No. 01KI1722A).

707

## 708 Data availability

709 The nucleotide sequences from this study are available from the INSDC databases study accession  
710 PRJEB47687.

## 711 References

712

- 713 Aberle, S. W., et al. (2018), 'Increase in human West Nile and Usutu virus infections, Austria, 2018',  
714 *Eurosurveillance*, 23 (43), 7-12.
- 715 Aguilera-Sepulveda, P., et al. (2021), 'A new cluster of West Nile virus lineage 1 isolated from a  
716 northern goshawk in Spain', *Transboundary and Emerging Disease*.
- 717 Aguilera-Sepulveda, P., et al. (2022), 'West Nile Virus Lineage 2 Spreads Westwards in Europe and  
718 Overwinters in North-Eastern Spain (2017-2020)', *Viruses-Basel*, 14 (3).
- 719 Anez, G., et al. (2013), 'Evolutionary dynamics of West Nile virus in the United States, 1999-2011:  
720 phylogeny, selection pressure and evolutionary time-scale analysis', *PLoS Neglected Tropical*  
721 *Diseases*, 7 (5), e2245.
- 722 Bakran-Lebl, K., et al. (2021), 'Diversity of West Nile and Usutu virus strains in mosquitoes at an  
723 international airport in Austria', *Transboundary and Emerging Diseases*, 1-14.
- 724 Balaban, M., et al. (2019), 'TreeCluster: Clustering biological sequences using phylogenetic trees',  
725 *Plos One*, 14 (8), e0221068.
- 726 Bardos, V., et al. (1959), 'Neutralizing antibodies against some neurotropic viruses determined in  
727 human sera in Albania', *Journal of Hygiene, Epidemiology, Microbiology and Immunology*, 3  
728 (3), 277-82.
- 729 Barzon, L., et al. (2015), 'Phylogenetic characterization of Central/Southern European lineage 2 West  
730 Nile virus: analysis of human outbreaks in Italy and Greece, 2013-2014', *Clinical Microbiology*  
731 *and Infection*, 21 (12), 1122.e1-22.e10.
- 732 Bodenhofer, U., Kothmeier, A., and Hochreiter, S. (2011), 'APCluster: an R package for affinity  
733 propagation clustering', *Bioinformatics*, 27 (17), 2463-64.
- 734 Brown, E. B. E., et al. (2012), 'Assessing the Risks of West Nile Virus-Infected Mosquitoes from  
735 Transatlantic Aircraft: Implications for Disease Emergence in the United Kingdom', *Vector-*  
736 *Borne and Zoonotic Diseases*, 12 (4), 310-20.
- 737 Busch, A., et al. (2020), 'Using affinity propagation clustering for identifying bacterial clades and  
738 subclades with whole-genome sequences of *Francisella tularensis*', *Plos Neglected Tropical*  
739 *Diseases*, 14 (9), e0008018.
- 740 Camp, J. V. and Nowotny, N. (2020), 'The knowns and unknowns of West Nile virus in Europe: what  
741 did we learn from the 2018 outbreak?', *Expert Review of Anti-Infective Therapy*, 18 (2), 145-  
742 54.
- 743 Campbell, K., et al. (2022), 'Making genomic surveillance deliver: A lineage classification and  
744 nomenclature system to inform rabies elimination', *PLoS Pathog*, 18 (5), e1010023.
- 745 Cellinese, N., Baum, D. A., and Mishler, B. D. (2012), 'Species and phylogenetic nomenclature', *Syst*  
746 *Biol*, 61 (5), 885-91.
- 747 Chaintoutis, S. C., et al. (2019), 'Evolutionary dynamics of lineage 2 West Nile virus in Europe, 2004-  
748 2018: Phylogeny, selection pressure and phylogeography', *Molecular Phylogenetics and*  
749 *Evolution*, 141, 106617.
- 750 Cheng, L., et al. (2013), 'Hierarchical and Spatially Explicit Clustering of DNA Sequences with BAPS  
751 Software', *Molecular Biology and Evolution*, 30 (5), 1224-28.
- 752 Cotar, A. I., et al. (2018), 'West Nile virus lineage 2 in Romania, 2015-2016: co-circulation and strain  
753 replacement', *Parasites & Vectors*, 11 (562).
- 754 Darriba, D., et al. (2012), 'jModelTest 2: more models, new heuristics and parallel computing', *Nature*  
755 *Methods*, 9 (8), 772-72.

- 756 Davis, C. T., et al. (2005), 'Phylogenetic analysis of North American West Nile virus isolates, 2001-  
757 2004: evidence for the emergence of a dominant genotype', *Virology*, 342 (2), 252-65.
- 758 Deutscher Wetterdienst (2021), 'Climatological maps of Germany',  
759 <https://www.dwd.de/EN/ourservices/klimakartendeutschland/klimakartendeutschland.htm>  
760 [?nn=495490](https://www.dwd.de/EN/ourservices/klimakartendeutschland/klimakartendeutschland.htm?nn=495490)>, accessed 15.07.2021.
- 761 Di Giallonardo, F., et al. (2016), 'Fluid Spatial Dynamics of West Nile Virus in the United States: Rapid  
762 Spread in a Permissive Host Environment', *Journal of Virology*, 90 (2), 862-72.
- 763 Drummond, A. J. and Rambaut, A. (2007), 'BEAST: Bayesian evolutionary analysis by sampling trees',  
764 *BMC Evolutionary Biology*, 7, 214.
- 765 Edgar, R. C. (2004), 'MUSCLE: a multiple sequence alignment method with reduced time and space  
766 complexity', *BMC Bioinformatics*, 5 (1), 113.
- 767 Eiden, Martin, et al. (2010), 'Two new real-time quantitative reverse transcription polymerase chain  
768 reaction assays with unique target sites for the specific and sensitive detection of lineages 1  
769 and 2 West Nile virus strains', *Journal of Veterinary Diagnostic Investigation*, 22 (5), 748–53
- 770 Eritja, R., et al. (2017), 'Direct Evidence of Adult Aedes albopictus Dispersal by Car', *Scientific Reports*,  
771 7 (1).
- 772 European Centre for Disease Prevention and Control (2019), 'West Nile virus infection', *ECDC: Annual*  
773 *epidemiological report for 2018* (Stockholm: ECDC).
- 774 --- (2022), 'West Nile virus in Europe in 2020 - human cases, updated 19 November',  
775 [https://www.ecdc.europa.eu/en/publications-data/west-nile-virus-europe-2020-human-](https://www.ecdc.europa.eu/en/publications-data/west-nile-virus-europe-2020-human-cases-updated-19-november)  
776 [cases-updated-19-november](https://www.ecdc.europa.eu/en/publications-data/west-nile-virus-europe-2020-human-cases-updated-19-november)>, accessed 24.02.2022.
- 777 --- (2021), 'Surveillance Atlas of Infectious Diseases',  
778 <http://atlas.ecdc.europa.eu/public/index.aspx?Dataset=27&HealthTopic=60>>, accessed  
779 14.07.2021.
- 780 Fall, G., et al. (2017), 'Biological and phylogenetic characteristics of West African lineages of West  
781 Nile', *Plos Neglected Tropical Diseases*, 11 (11), e0006078.
- 782 Fischer, S., et al. (2018), 'Defining objective clusters for rabies virus sequences using affinity  
783 propagation clustering', *Plos Neglected Tropical Diseases*, 12 (1), e0006182.
- 784 Frank, C., et al. (2022), 'West Nile Virus in Germany: An Emerging Infection and Its Relevance for  
785 Transfusion Safety', *Transfusion Medicine and Hemotherapy*.
- 786 Frey, B. J. and Dueck, D. (2007), 'Clustering by passing messages between data points', *Science*, 315  
787 (5814), 972-76.
- 788 Goya, S., et al. (2020), 'Toward unified molecular surveillance of RSV: A proposal for genotype  
789 definition', *Influenza Other Respir Viruses*, 14 (3), 274-85.
- 790 Hadfield, J., et al. (2019), 'Twenty years of West Nile virus spread and evolution in the Americas  
791 visualized by Nextstrain', *Plos Pathogens*, 15 (10), e1008042.
- 792 Han, A. X., et al. (2019), 'Phylogenetic Clustering by Linear Integer Programming (PhyCLIP)', *Molecular*  
793 *Biology and Evolution*, 36 (7), 1580-95.
- 794 Hoang, D. T., et al. (2018), 'UFBoot2: Improving the Ultrafast Bootstrap Approximation', *Molecular*  
795 *Biology and Evolution*, 35 (2), 518-22.
- 796 Holicki, C. M., et al. (2020), 'West Nile Virus Lineage 2 Vector Competence of Indigenous Culex and  
797 Aedes Mosquitoes from Germany at Temperate Climate Conditions', *Viruses*, 12 (5).
- 798 ICTV (2022), 'Genus: Flavivirus', *The ICTV Report on Virus Classification and Taxon Nomenclature*  
799 (updated October 2020) [https://talk.ictvonline.org/ictv-reports/ictv\\_online\\_report/positive-](https://talk.ictvonline.org/ictv-reports/ictv_online_report/positive-sense-rna-viruses/w/flaviviridae)  
800 [sense-rna-viruses/w/flaviviridae](https://talk.ictvonline.org/ictv-reports/ictv_online_report/positive-sense-rna-viruses/w/flaviviridae)>, accessed 25.02.2022.
- 801 Jungbauer, C., et al. (2015), 'West Nile virus lineage 2 infection in a blood donor from Vienna, Austria,  
802 August 2014', *Journal of Clinical Virology*, 64, 16-19.
- 803 Kampen, H., et al. (2020), 'West Nile Virus Mosquito Vectors (Diptera: Culicidae) in Germany',  
804 *Viruses*, 12 (5), 493.
- 805 Kass, Robert E. and Raftery, Adrian E. (1995), 'Bayes factor and model uncertainty.', *Journal of the*  
806 *American Statistical Association*, 90 (430), 773-95.
- 807 Kolodziejek, J., et al. (2014), 'The Complete Sequence of a West Nile Virus Lineage 2 Strain Detected  
808 in a Hyalomma marginatum marginatum Tick Collected from a Song Thrush (Turdus

- 809 philomelos) in Eastern Romania in 2013 Revealed Closest Genetic Relationship to Strain  
810 Volgograd 2007', *Plos One*, 9 (10), e109905.
- 811 Kolodziejek, J., et al. (2015), 'West Nile Virus Positive Blood Donation and Subsequent Entomological  
812 Investigation, Austria, 2014', *Plos One*, 10 (5).
- 813 Kolodziejek, J., et al. (2018), 'Integrated analysis of human-animal-vector surveillance: West Nile virus  
814 infections in Austria, 2015-2016', *Emerging Microbes & Infections*, 7 (1), 1-15.
- 815 Kuno, Goro, et al. (1998), 'Phylogeny of the Genus *Flavivirus*', *Journal of Virology*, 72 (1), 73-83.
- 816 Mann, B. R., et al. (2013), 'Molecular Epidemiology and Evolution of West Nile Virus in North  
817 America', *International Journal of Environmental Research and Public Health*, 10 (10), 5111-  
818 29.
- 819 May, F. J., et al. (2011), 'Phylogeography of West Nile Virus: from the Cradle of Evolution in Africa to  
820 Eurasia, Australia, and the Americas', *Journal of Virology*, 85 (6), 2964-74.
- 821 McMullen, A. R., et al. (2013), 'Molecular evolution of lineage 2 West Nile virus', *Journal of General  
822 Virology*, 94, 318-25.
- 823 Mencattelli, G., et al. (2022), 'Epidemiology of West Nile virus in Africa: An underestimated threat',  
824 *PLoS Negl Trop Dis*, 16 (1), e0010075.
- 825 Michel, Friederike, et al. (2018), 'West Nile Virus and Usutu Virus Monitoring of Wild Birds in  
826 Germany', *International Journal of Environmental Research and Public Health*, 15 (1), 171.
- 827 Michel, Friederike, et al. (2019), 'Evidence for West Nile Virus and Usutu Virus Infections in Wild and  
828 Resident Birds in Germany, 2017 and 2018', *Viruses*, 11 (7), 674.
- 829 Minh, B. Q., Nguyen, M. A., and von Haeseler, A. (2013), 'Ultrafast approximation for phylogenetic  
830 bootstrap', *Molecular Biology and Evolution*, 30 (5), 1188-95.
- 831 Minh, B. Q., et al. (2022), 'IQ-TREE version 2.2.0: Tutorials and Manual  
832 Phylogenomic software by maximum likelihood', <<http://www.iqtree.org/doc/iqtree-doc.pdf>>,  
833 accessed 15.09.2022.
- 834 Mishler, B. D. (2010), 'Species are not uniquely real biological entities', in F. J. Ayala and R. Arp (eds.),  
835 *Contemporary Debates in Philosophy of Biology* (Malden (MA): Wiley-Blackwell), 110-22.
- 836 Muhire, B. M., Varsani, A., and Martin, D. P. (2014), 'SDT: A Virus Classification Tool Based on  
837 Pairwise Sequence Alignment and Identity Calculation', *Plos One*, 9 (9).
- 838 Murgue, B., et al. (2001), 'West Nile outbreak in horses in Southern France, 2000: The return after 35  
839 years', *Emerging Infectious Diseases*, 7 (4), 692-96.
- 840 Nguyen, L. T., et al. (2015), 'IQ-TREE: a fast and effective stochastic algorithm for estimating  
841 maximum-likelihood phylogenies', *Molecular Biology and Evolution*, 32 (1), 268-74.
- 842 Pachler, K., et al. (2014), 'Putative new West Nile virus lineage in *Uranotaenia unguiculata*  
843 mosquitoes, Austria, 2013', *Emerg Infect Dis*, 20 (12), 2119-22.
- 844 Paull, S. H., et al. (2017), 'Drought and immunity determine the intensity of West Nile virus epidemics  
845 and climate change impacts', *Proceedings of the Royal Society B-Biological Sciences*, 284  
846 (1848).
- 847 Perez-Ramirez, E., et al. (2017), 'Pathogenicity evaluation of twelve West Nile virus strains belonging  
848 to four lineages from five continents in a mouse model: discrimination between three  
849 pathogenicity categories', *J Gen Virol*, 98 (4), 662-70.
- 850 Pietsch, C., et al. (2020), 'Autochthonous West Nile virus infection outbreak in humans, Leipzig,  
851 Germany, August to September 2020', *Eurosurveillance*, 25 (46).
- 852 Quick, J., et al. (2017), 'Multiplex PCR method for MinION and Illumina sequencing of Zika and other  
853 virus genomes directly from clinical samples', *Nature Protocols*, 12 (6), 1261-76.
- 854 R Core Team (2022), 'R: A language and environment for statistical computing', <[https://www.R-  
855 project.org/](https://www.R-project.org/)>, accessed 12.09.2022.
- 856 Ragonnet-Cronin, M., et al. (2013), 'Automated analysis of phylogenetic clusters', *Bmc Bioinformatics*,  
857 14 (1).
- 858 Rambaut, A., et al. (2016), 'Exploring the temporal structure of heterochronous sequences using  
859 TempEst (formerly Path-O-Gen)', *Virus Evolution*, 2 (1).

- 860 Rambaut, A., et al. (2020), 'A dynamic nomenclature proposal for SARS-CoV-2 lineages to assist  
861 genomic epidemiology (vol 5, pg 1403, 2020)', *Nature Microbiology*, 5 (11), 1403–07.
- 862 Ravagnan, S., et al. (2015), 'First report outside Eastern Europe of West Nile virus lineage 2 related to  
863 the Volgograd 2007 strain, northeastern Italy, 2014', *Parasites & Vectors*, 8 (1).
- 864 Rizzoli, A., et al. (2015), 'The challenge of West Nile virus in Europe: knowledge gaps and research  
865 priorities', *Eurosurveillance*, 20 (20).
- 866 Robert-Koch-Institut (2020), 'Autochthone Infektionen mit dem West-Nil-Virus in Deutschland 2018  
867 und 2019', *Epidemiologisches Bulletin*, 25, 3-10.
- 868 Ronca, S. E., Ruff, J. C., and Murray, K. O. (2021), 'A 20-year historical review of West Nile virus since  
869 its initial emergence in North America: Has West Nile virus become a neglected tropical  
870 disease?', *Plos Neglected Tropical Diseases*, 15 (5).
- 871 Rudolf, I., et al. (2014), 'West Nile virus lineage 2 isolated from *Culex modestus* mosquitoes in the  
872 Czech Republic, 2013: expansion of the European WNV endemic area to the North?',  
873 *Eurosurveillance*, 19 (31), 2-5.
- 874 Savage, H. M., et al. (1999), 'Entomologic and avian investigations of an epidemic of West Nile fever  
875 in Romania in 1996, with serologic and molecular characterization of a virus isolate from  
876 mosquitoes', *American Journal of Tropical Medicine and Hygiene*, 61 (4), 600-11.
- 877 Schneider, J., et al. (2021), 'Autochthonous West Nile virus infection in Germany: Increasing numbers  
878 and a rare encephalitis case in a kidney transplant recipient', *Transboundary and Emerging  
879 Disease*, 1-6.
- 880 Sedlak, K., et al. (2014), 'Surveillance of West Nile fever in horses in the Czech Republic from 2011 to  
881 2013', *Epidemiologie Mikrobiologie Immunologie*, 63 (4), 307-11.
- 882 Sikkema, R. S., et al. (2020), 'Detection of West Nile virus in a common whitethroat (*Curruca  
883 communis*) and *Culex* mosquitoes in the Netherlands, 2020', *Eurosurveillance*, 25 (40).
- 884 Simmonds, P., et al. (2017), 'ICTV Virus Taxonomy Profile: Flaviviridae', *Journal of General Virology*,  
885 98 (1), 2-3.
- 886 Smithburn, K. C., et al. (1940), 'A neurotropic virus isolated from the blood of a native of Uganda',  
887 *The American Journal of Tropical Medicine and Hygiene*, s1-20 (4), 471-92.
- 888 Suchard, M. A., et al. (2018), 'Bayesian phylogenetic and phylodynamic data integration using BEAST  
889 1.10', *Virus Evolution*, 4 (1), vey016.
- 890 Tsai, T. F., et al. (1998), 'West Nile encephalitis epidemic in southeastern Romania', *Lancet*, 352  
891 (9130), 767-71.
- 892 Ulbert, S. (2019), 'West Nile virus vaccines - current situation and future directions', *Human Vaccines  
893 & Immunotherapeutics*, 15 (10), 2337-42.
- 894 Vlckova, J., et al. (2015), 'West Nile virus transmission risk in the Czech Republic', *Epidemiologie  
895 Mikrobiologie Immunologie*, 64 (2), 80-86.
- 896 Wylezich, C., et al. (2018), 'A Versatile Sample Processing Workflow for Metagenomic Pathogen  
897 Detection', *Scientific Reports*, 8 (1), 13108.
- 898 Wylezich, C., et al. (2021), 'Next-generation diagnostics: virus capture facilitates a sensitive viral  
899 diagnosis for epizootic and zoonotic pathogens including SARS-CoV-2', *Microbiome*, 9 (1), 51.
- 900 Zehender, G., et al. (2017), 'Reconstructing the recent West Nile virus lineage 2 epidemic in Europe  
901 and Italy using discrete and continuous phylogeography', *Plos One*, 12 (7).
- 902 Ziegler, U., et al. (2019), 'West Nile virus epizootic in Germany, 2018', *Elsevier*, 162, 39-43.
- 903 Ziegler, U., et al. (2020), 'West Nile Virus Epidemic in Germany Triggered by Epizootic Emergence,  
904 2019', *Viruses*, 12 (4).
- 905 Ziegler, U., et al. (2022), 'Spread of West Nile Virus and Usutu Virus in the German Bird Population,  
906 2019-2020', *Microorganisms*, 10 (4).



**Table 1** Overview of WNV cases analyzed in this study. Sample numbers are used in Figures 4 and 7.

Sample no.	Sample ID	Library ID	Sequence accession	Common English name	Scientific name	Collection date	Federal state <sup>1</sup>
1	167/20	lib04566		Blue tit	<i>Cyanistes caeruleus</i>	07.07.2020	BE
2	174/20	lib04567		Snowy owl	<i>Bubo scandiacus</i>	12.07.2020	TH
3	192/20	lib04568		Snowy owl	<i>Bubo scandiacus</i>	15.08.2020	TH
4	193/20	lib04569		Northern goshawk	<i>Accipiter gentilis</i>	30.07.2020	SN
5	200/20	lib04570		Bohemian waxwing	<i>Bombycilla garrulus</i>	11.08.2020	BB
6	203/20	lib04571		Little owl	<i>Athene noctua</i>	18.08.2020	BB
7	206/20	lib04572		Northern goshawk	<i>Accipiter gentilis</i>	08.08.2020	BE
8	214/20	lib04573		Unspecified flamingo	<i>Phoenicopterus sp.</i>	19.08.2020	TH
9	218/20	lib04574		Unspecified flamingo	<i>Phoenicopterus sp.</i>	18.08.2020	ST
10	339/20	lib04575		Chilean flamingo	<i>Phoenicopterus chilensis</i>	25.08.2020	BE
11	252/20	lib04576		Eurasian jay	<i>Garrulus glandarius</i>	Aug./Sept.2020	TH
12	283/20	lib04577		Snowy owl	<i>Bubo scandiacus</i>	02.09.2020	ST
13	207/20	lib04717		Northern goshawk	<i>Accipiter gentilis</i>	09.08.2020	BE
14	208/20	lib04718		Northern goshawk	<i>Accipiter gentilis</i>	14.08.2020	BB
15	211/20	lib04719		Blue tit	<i>Cyanistes caeruleus</i>	August 2020	BE
16	194/20	lib04720		Blue tit	<i>Cyanistes caeruleus</i>	August 2020	SN
17	268/20 Nr. 1	lib04721		Little owl	<i>Athene noctua</i>	September 2020	BB
18	311/20	lib04722		Northern goshawk	<i>Accipiter gentilis</i>	Sept./Okt. 2020	BE
19	314/20	lib04723		Northern goshawk	<i>Accipiter gentilis</i>	Sept./Okt. 2020	BE
20	315/20	lib04724		Northern goshawk	<i>Accipiter gentilis</i>	Sept./Okt. 2020	BE
21	224/20	lib04725		Blue tit	<i>Cyanistes caeruleus</i>	August 2020	BE
22	282/20	lib04726		Snowy owl	<i>Bubo scandiacus</i>	02.09.2020	ST
23	281/20	lib04727		Unspecified flamingo	<i>Phoenicopterus sp.</i>	September 2020	ST
24	340/20	lib04728		American flamingo	<i>Phoenicopterus ruber</i>	22.08.2020	BE
25	196/20	lib04729		Unspecified buzzard	<i>Buteo sp.</i>	August 2020	SN
26	258/20	lib04730		Great tit	<i>Parus major</i>	Aug./Sept.2020	SN
27	242/20	lib04731		Northern goshawk	<i>Accipiter gentilis</i>	August 2020	BE
28	245/20	lib04732		Unspecified flamingo	<i>Phoenicopterus sp.</i>	August 2020	BE
29	260/20	lib04733		Domestic canary	<i>Serinus canaria forma domestica</i>	September 2020	ST

Sample no.	Sample ID	Library ID	Sequence accession	Common English name	Scientific name	Collection date	Federal state <sup>1</sup>
30	261/20	lib04734		Chilean flamingo	<i>Phoenicopterus chilensis</i>	September 2020	SN
31	264/20	lib04735		Unspecified sparrow	<i>Passer sp.</i>	September 2020	SN
32	228/20	lib04736		Horse	<i>Equus caballus</i>	02.09.2020	SN
33	173/20	lib04737		Alpine chough	<i>Pyrrhocorax graculus</i>	12.07.2020	ST
34	216/20	lib04738		Blue tit	<i>Cyanistes caeruleus</i>	August 2020	TH
35	199/20	lib04739		Northern goshawk	<i>Accipiter gentilis</i>	13.06.2020	BE
36	205/20	lib04740		Northern goshawk	<i>Accipiter gentilis</i>	13.08.2020	BE
37	210/20	lib04741		Northern goshawk	<i>Accipiter gentilis</i>	01.08.2020	BE
38	238/20	lib04742		Northern goshawk	<i>Accipiter gentilis</i>	31.08.2020	BE
39	241/20	lib04743		Northern goshawk	<i>Accipiter gentilis</i>	23.08.2020	BE
40	244/20	lib04744		Hooded crow	<i>Corvus corone cornix</i>	18.08.2020	BE
41	219/20	lib04745		Chilean flamingo	<i>Phoenicopterus chilensis</i>	26.08.2020	ST
42	284/20	lib04746		Swift parrot	<i>Lathamus discolor</i>	21.09.2020	ST
43	286/20	lib04747		Horse	<i>Equus caballus</i>	29.09.2020	ST
44	246/20	lib04757		Golden eagle	<i>Aquila chrysaetos</i>	(09.09.2020) survived	BB
45	201/20	na <sup>2</sup>		European greenfinch	<i>Carduelis chloris</i>	07.07.2020	BB
46	60/21	lib04758		Blue tit	<i>Cyanistes caeruleus</i>	2020	TH
C4	115/19	lib04565		Chinese merganser	<i>Mergus squamatus</i>	08.08.2019	BE
C5	127/18	lib04748		Horse	<i>Equus caballus</i>	11.09.2018	BB

909 <sup>1</sup> Abbreviations for federal states: BE, Berlin; BB, Brandenburg; SN, Saxony; ST, Saxony Anhalt; TH, Thuringia

910 <sup>2</sup> WNV-specific multiplex PCR was unsuccessful due to low amount of WNV-RNA in the sample (Cq 36).

911 **Table 2** Overview of terms commonly used for the designation of virus sequences into groups below the species rank.

Term	General definition	Current common use in the WNV research community			Proposed use	
		Definition	Example lineage 1	Example lineage 2	Level below species/term	Example designation
Lineage	Rank-independent term for the relationships between ancestors and descendants through time (diachronic). Typically, a higher resolution classification compared to clade. (Campbell et al. 2022; Cellinese et al. 2012; Rambaut et al. 2020)	Broadest monophyletic group below the WNV species rank. There are 9 proposed WNV lineages. (Fall et al. 2017)	Lineage 1; Lineage 1a	Lineage 2	1 / Lineage	Lineage 1; Lineage 2
Clade	Rank-independent term for a monophyletic group on a phylogenetic tree. Mishler (2010), describe it as "a monophyletic group is all and only the descendants of common ancestors" (synchronic). (Campbell et al. 2022; Cellinese et al. 2012; Rambaut et al. 2020)	Smaller monophyletic group within the lineage. Typically denoted with letters. Example, 1a - 1c and 2a-2d (May et al. 2011; McMullen et al. 2013). In Lineage 2, this level also describes a monophyletic group sharing similar geographic range. (Ziegler et al. 2020)	Clade 1a	Clade 2d; Central/Southern European clade	2 / Clade	Clade 1.1; Clade 2.5
Subclade	A smaller monophyletic group within a larger clade (Campbell et al. 2022)	Smaller monophyletic group within the clade. More often used in Lineage 2. In Lineage 2, these are also used to describe sequences from a monophyletic branch sharing geographic range. (Barzon et al. 2015; Ziegler et al. 2020)	Not commonly used in Lineage 1	Central/Southern European subclade; subclade: "Eastern German clade"	3 / Subclade	Subclade 1.1.4; Subclade 2.5.1

Term	General definition	Current common use in the WNV research community			Proposed use	
		Definition	Example lineage 1	Example lineage 2	Level below species/term	Example designation
Cluster	Closely related sequences sharing a certain threshold of nucleotide or amino acid identities, characteristics, or provides to define cluster of disease transmission. (Han et al. 2019)	Smaller monophyletic group within the clade in Lineage 1, sharing a single ancestor and or a fixed unique non-synonymous mutation (May et al). Smaller monophyletic group within the clade or subclade in Lineage 2. (Barzon et al. 2015)	Cluster 1	Italian Lombardy cluster	4 / Cluster	Cluster 1.1.4.1 or Subclade 1.1.4 cluster 1; Cluster 2.5.1.1 or Subclade 2.5.1 cluster 1
Subtype	A subset of a species based on a certain characteristic	Below Cluster level, to designate WNV cluster 2 based on geographic location. (May et al. 2011)	Mediterranean subtype (cluster 2)	not commonly used in Lineage 2	5 / Subcluster (designated by 5 <sup>th</sup> decimal place)	Subcluster 1.1.4.1.6; Subcluster 2.5.1.1.5
Genotype	monophyletic cluster of sequences with high statistical support (Goya et al. 2020)	Used to describe different sequences of WNV lineage 1 cluster 4 detected in America, which shared fixed nonsynonymous mutation. Sub-type was not described in cluster 4 (Mann et al. 2013).	NY99 genotype (cluster 4)	not commonly used in Lineage 2	6 / Subcluster (designated by a letter as suffix)	Subcluster 1.1.4.1.6a; Subcluster 2.5.1.1.5a

912

913

914 **Table 3** Summary of avian species infected with WNV in 2020 in Germany

Order	Common English Name	Scientific Name	Housing	Number	Affected Federal State <sup>1</sup>	
<i>Accipitriformes</i>	Unspecified buzzard	<i>Buteo sp.</i>	wild	1	SN	
	Northern goshawk	<i>Accipiter gentilis</i>	wild/captive	17	BE, BB, SN	
	Golden eagle	<i>Aquila chrysaetos</i>	captive	1	BB	
<i>Charadriiformes</i>	Black-tailed gull	<i>Larus crassirostris</i>	captive	1	BE	
<i>Passeriformes</i>	Alpine chough	<i>Pyrrhocorax graculus</i>	captive	1	ST	
	Blue tit	<i>Parus caeruleus</i>	wild	8	BE, SN, TH	
	Eurasian jay	<i>Garrulus glandarius</i>	wild	1	TH	
	European greenfinch	<i>Carduelis chloris</i>	wild	1	BB	
	Domestic canary	<i>Serinus canaria forma domestica</i>	captive	1	ST	
	Great tit	<i>Parus major</i>	wild	1	SN	
	Hooded crow	<i>Corvus corone cornix</i>	wild	2	BE	
	Bohemian waxwing	<i>Bombycilla garrulus</i>	captive	1	BB	
	Unspecified sparrow	<i>Passer sp.</i>	wild	1	SN	
	<i>Phoenicopteriformes</i>	Chilean flamingo	<i>Phoenicopterus chilensis</i>	captive	6	BE, ST, SN
		American flamingo	<i>Phoenicopterus ruber</i>	captive	1	BE
		Unspecified flamingo	<i>Phoenicopterus sp.</i>	captive	8	BE, ST, TH
	<i>Psittaciformes</i>	Swift parrot	<i>Lathamus discolor</i>	captive	2	ST
<i>Strigiformes</i>	Snowy owl	<i>Bubo scandiacus</i>	captive	4	ST, TH	
	Little owl	<i>Athene noctua</i>	captive	5	BB	
	Barn owl	<i>Tyto alba</i>	wild	1	BB	
	Eurasian eagle-owl	<i>Bubo bubo</i>	captive	1	ST	

915 <sup>1</sup> Abbreviations for federal states: BE, Berlin; BB, Brandenburg; SN, Saxony; ST, Saxony Anhalt; TH, Thuringia

916 **Figure legends**

917

918 **Figure 1** Graphical representation of the proposed hierarchy and the corresponding group labels.

919 The levels of the proposed are ordered top to bottom; the corresponding group label is organized left  
920 to right. Note that the subcluster can either have the number only or the number combined with a  
921 letter.

922

923 **Figure 2** Comparison of APC groupings of test dataset TD03 with previously defined groupings and  
924 phylogenetic reconstruction.

925 The representation of the objective APC grouping includes the addressed hierarchical levels, starting  
926 with lineage, decreasing from left to right down to the subclade. The vertical lines mark the final level  
927 down to which the grouping could be done (limited either by the minimum group size applied for the  
928 input of subgrouping or by the hierarchical level that was the last to be shown). Horizontal lines  
929 separate the individual groups. Each group is labelled at the right-hand side of the graph. Dashed  
930 vertical lines with arrows connect areas of the graph together forming one common group  
931 interspersed by other group(s). The horizontal grey rectangle labelled "X" marks a sequence that was  
932 not considered for APC/AHC grouping due to its high number of ambiguities ( $\geq 10$ ). For comparison,  
933 the groupings that were previously published by Fall et al. (2017) and May et al. (2011) are included.  
934 Here, a filled circle represents a singleton sequence making up the respective group as labelled and  
935 two filled circles connected by a vertical line represent a larger group. White rectangles mark  
936 sequences included in the tree but not part of the cited analyses. The maximum likelihood (ML)  
937 phylogenetic analysis of sequences from TD03 was done with the best fitting model GTR+I+G and  
938 100,000 ultrafast bootstraps. Few large branches consisting of sequences from almost the same  
939 geographic regions are collapsed into triangles. The nodes are labelled with ultrafast bootstrap values.

940

941 **Figure 3** Comparison of APC groupings of WNV lineage 2 (WL2) sequences with previously defined  
942 groupings and phylogenetic reconstruction.

943 The representation of the objective APC grouping includes the addressed hierarchical levels, starting  
944 with lineage (not calculated here but WNV lineage 2 sequences included according to published  
945 references), decreasing from left to right down to the cluster. The vertical lines mark the final level  
946 down to which the grouping could be done (limited either by the minimum group size applied for the  
947 input of subgrouping or by the hierarchical level that was the last to be shown). Horizontal lines  
948 separate the individual groups. Each group is labelled at the right-hand side of the graph. Dashed  
949 vertical lines with arrows connect areas of the graph together forming one common group  
950 interspersed by other group(s). The horizontal grey rectangle labelled “X” marks a sequence that was  
951 not considered for APC/AHC grouping due to its high number of ambiguities ( $\geq 10$ ). For comparison,  
952 the groupings that were previously published by Chaintoutis et al. (2019), McMullen et al. (2013),  
953 Ravagnan et al. (2015), Zehender et al. (2017) and Ziegler et al. (2020) are included. Here, a filled circle  
954 represents a singleton sequence making up the respective group as labelled and two filled circles  
955 connected by a vertical line represent a larger group. White rectangles mark sequences included in the  
956 tree but not part of the cited analyses. The maximum likelihood (ML) phylogenetic analysis of  
957 sequences from WL2 was done with the best fitting model GTR+I+G and 100,000 ultrafast bootstraps.  
958 Few large branches consisting of sequences from almost the same geographic regions are collapsed  
959 into triangles. The nodes are labelled with ultrafast bootstrap values.

960

961 **Figure 4** Bayesian maximum clade credibility (MCC) tree representing time scaled phylogeny of  
962 European WNV subclade 2.5.3 complete coding sequences together with objective APC groups.

963 WNV sequences acquired in this study are highlighted yellow. All other WNV sequences were retrieved  
964 from GenBank and are listed in Table S3. The colored branches of MCC trees represent the most  
965 probable geographic location of their descendants (see legend “locations”). Bayesian posterior  
966 probabilities are indicated at each node. Time (in years) is indicated as x-axis below the MCC tree. The  
967 time for the most recent common ancestor (MRCA), time intervals defined by the 95% highest  
968 posterior density (95% HPD), and posterior probabilities (pp) are shown in the following nodes that  
969 consist of the following WNV sequences: (i) LR743448 and MW036634, (ii) cluster 2.5.3.2 sequences,

970 and (iii) subcluster 2.5.3.4.3c sequences. The representation of the objective APC grouping includes  
971 the addressed hierarchical levels, starting with cluster decreasing from left to right down to the  
972 subcluster. The vertical lines mark the final level down to which the grouping could be done (limited  
973 either by the minimum group size applied for the input of subgrouping or by the hierarchical level that  
974 was the last to be shown). Horizontal lines separate the individual groups. Each group is labelled at the  
975 right-hand side of the graph. Dashed vertical lines with arrows connect areas of the graph together  
976 forming one common group interspersed by other group(s).

977

978 **Figure 5** Notifiable WNV-cases of birds and horses in Germany from 2018 –20.

979 The number of cases were summed up per federal state and year. Notifiable cases in horses and birds  
980 were represented by blue and red bars, respectively. Abbreviations of federal states in Germany: BB –  
981 Brandenburg, BE – Berlin, BY – Bavaria, HH – Hamburg, NI – Lower Saxony, MV - Mecklenburg Western  
982 Pomerania, SN – Saxony, ST – Saxony-Anhalt, and TH – Thuringia.

983

984 **Figure 6** Geographic distribution of WNV cases in Germany from 2018-20 per host and (sub)clusters.

985 Labelling according to the legend in the graph. WNV-positive cases confirmed by the National  
986 Reference Laboratory without complete coding sequences are depicted in grey (labelled  
987 “undetermined” in the legend).

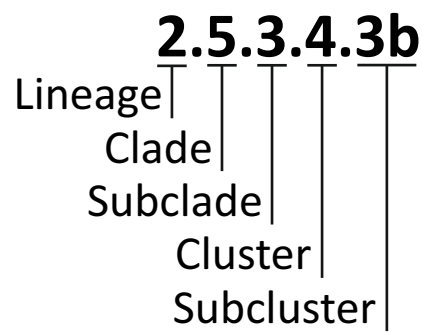
988

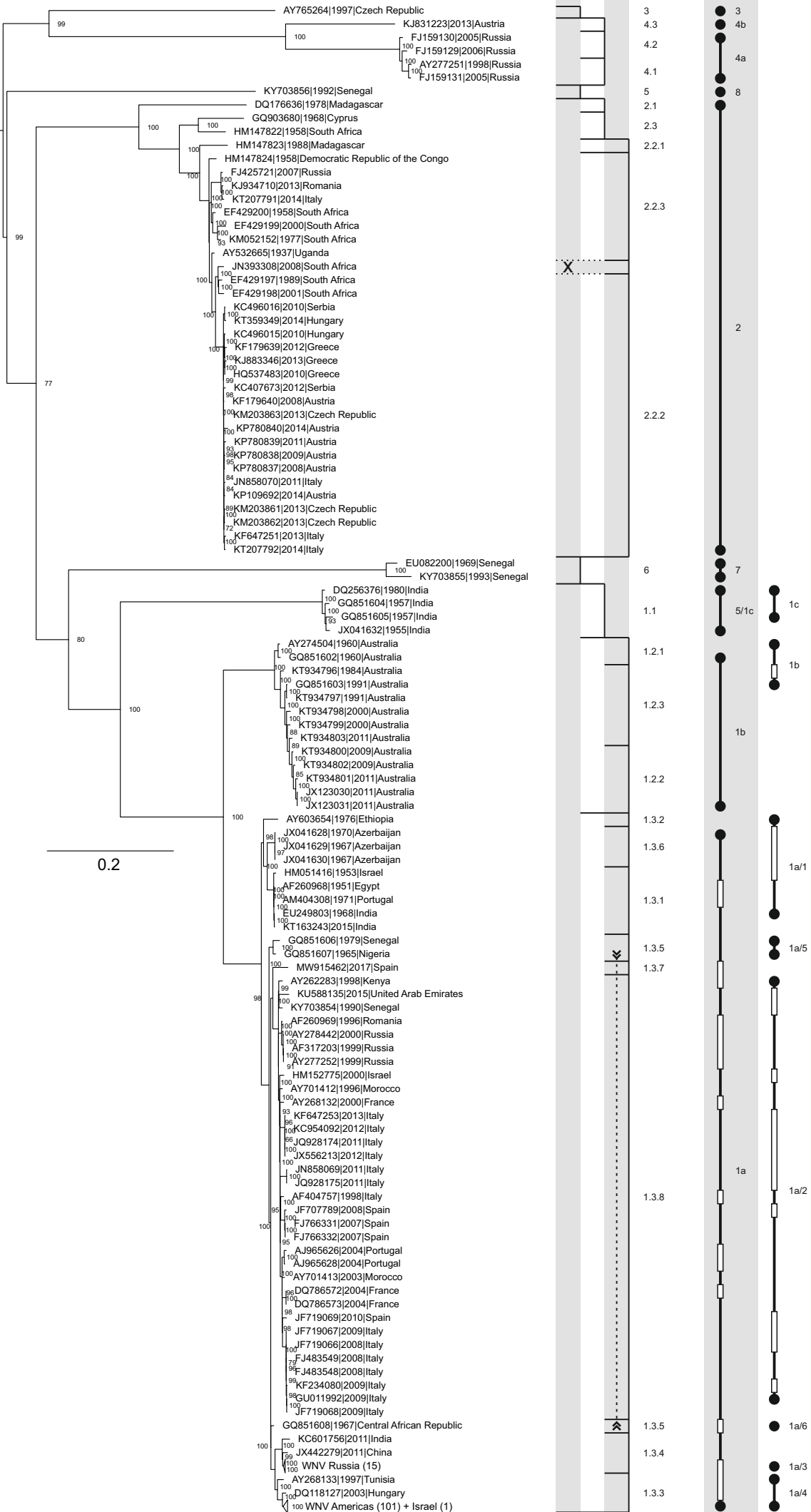
989 **Figure 7** Summarized geographic distribution of WNV cases in Germany from 2018 –20.

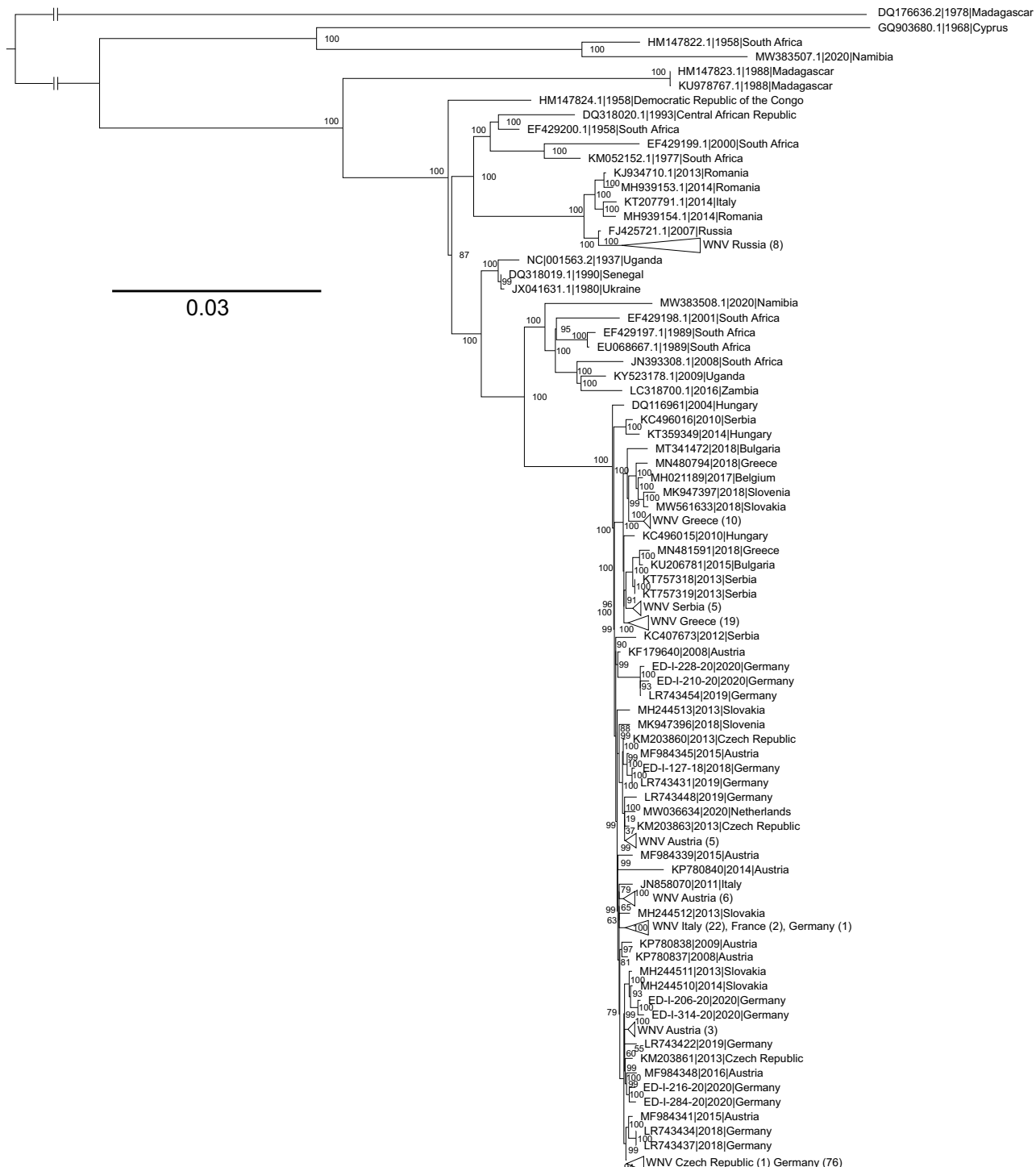
990 Labelling according to the legend in the graph. WNV-positive cases confirmed by the National  
991 Reference Laboratory without complete coding sequences are depicted in grey (labelled  
992 “undetermined” in the legend). Districts colored gray indicate areas with (additional) WNV-positive  
993 cases from WNV seasons 2018-19 without a complete coding sequence. Areas with high WNV activity  
994 in 2020 are shown in enlarged and separated maps, (B) Berlin, (C) Saxony, Saxony-Anhalt and Thuringia.  
995 New WNV cases from this study are indicated with numbers as described in Table 1.

996

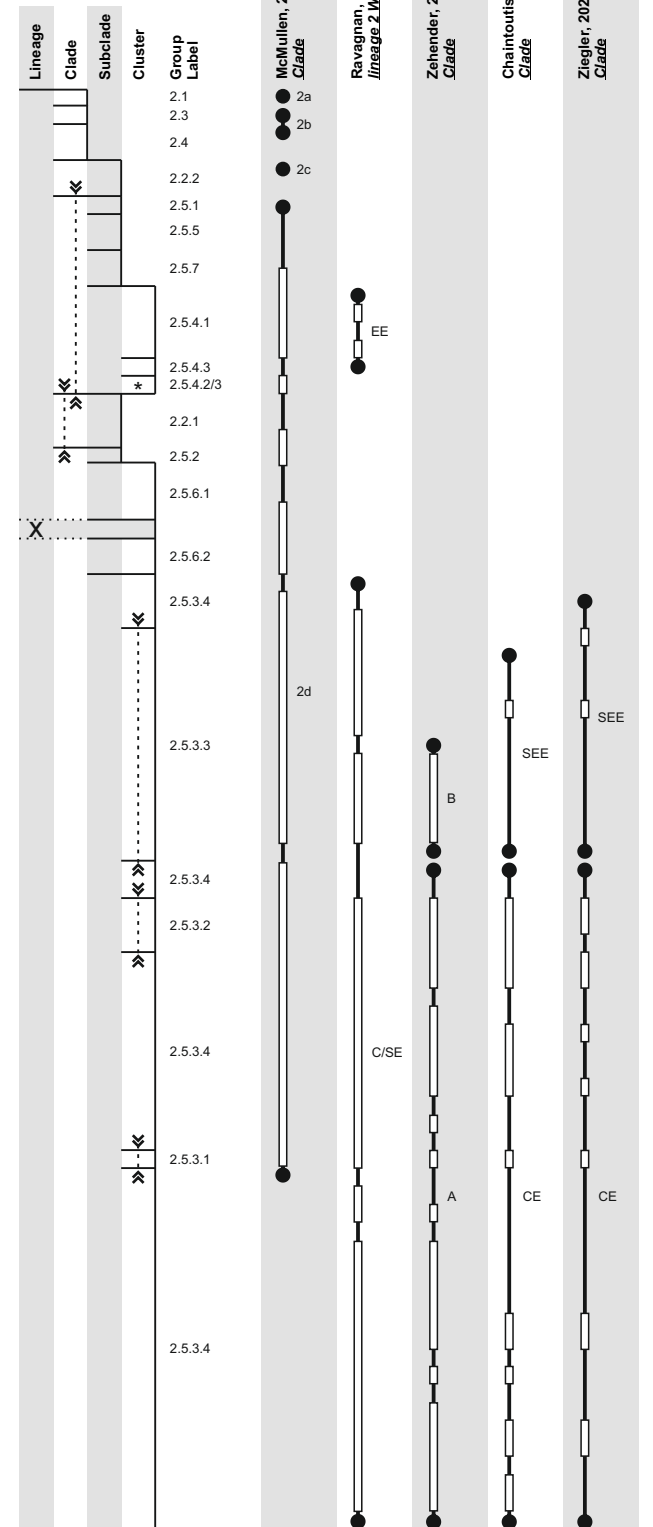


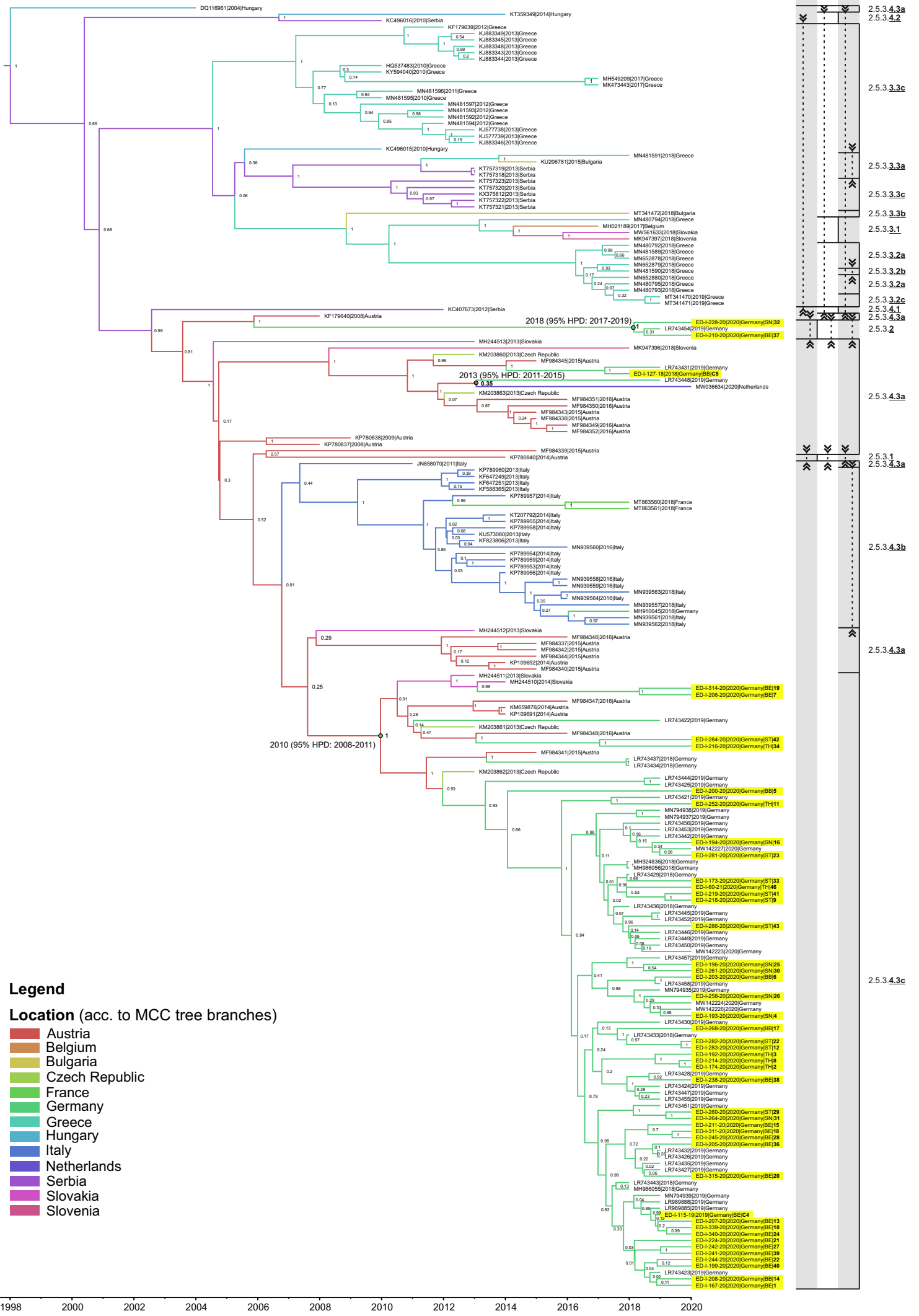


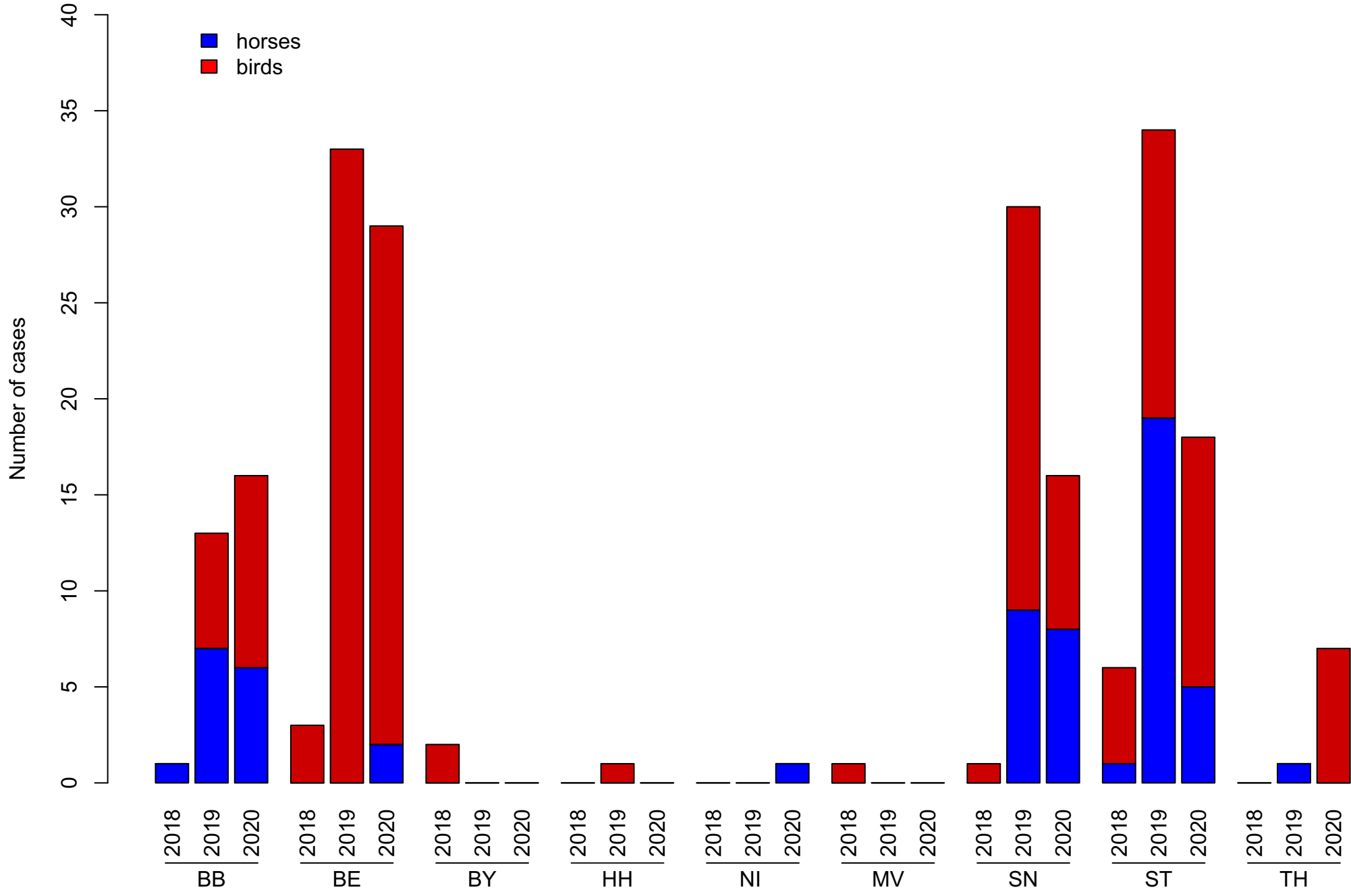


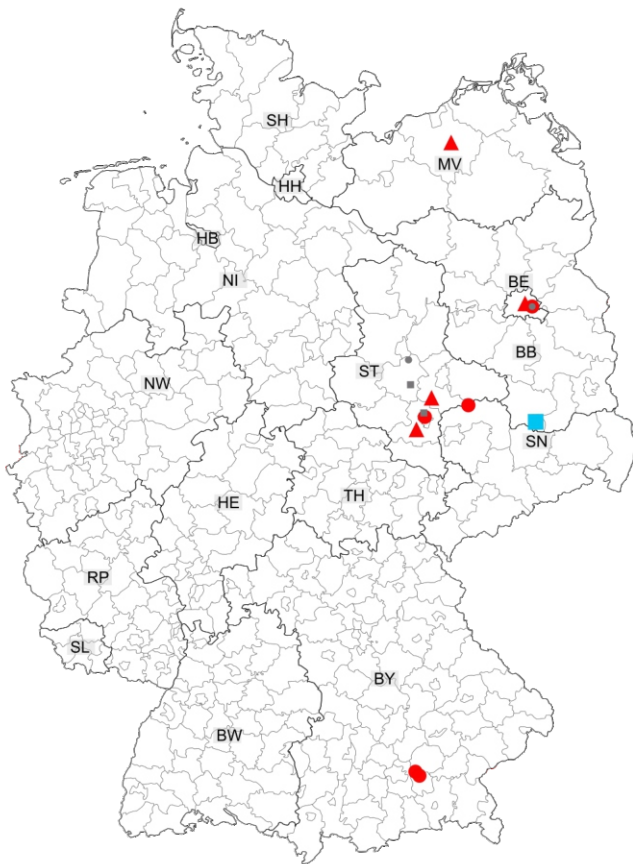


**Objective APC Grouping**

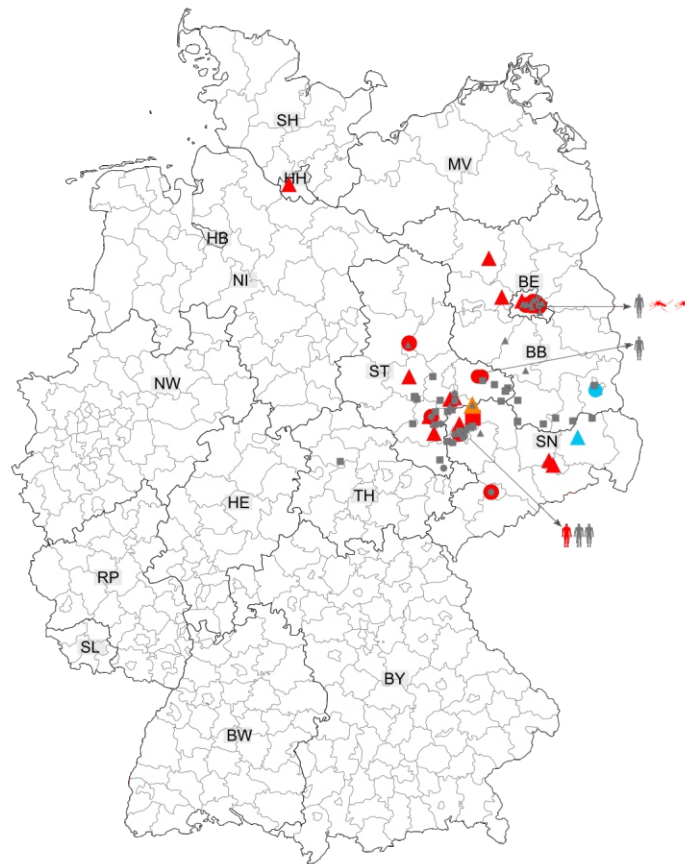




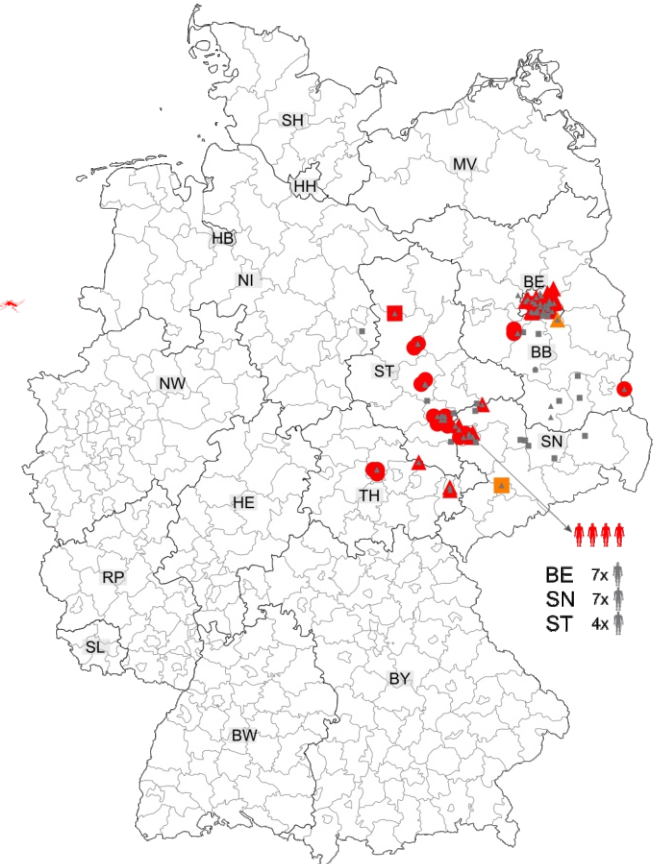




2018



2019



2020



**Legend**

**Federal States**





- |                                 |                             |
|---------------------------------|-----------------------------|
| BB – Brandenburg                | NI – Lower Saxony           |
| BE – Berlin                     | NW – North Rhine-Westphalia |
| BW – Baden-Württemberg          | RP – Rhineland-Palatinate   |
| BY – Bavaria                    | SH – Schleswig-Holstein     |
| HB – Bremen                     | SL – Saarland               |
| HE – Hesse                      | SN – Saxony                 |
| HH – Hamburg                    | ST – Saxony-Anhalt          |
| MV – Mecklenburg-West Pomerania | TH – Thuringia              |

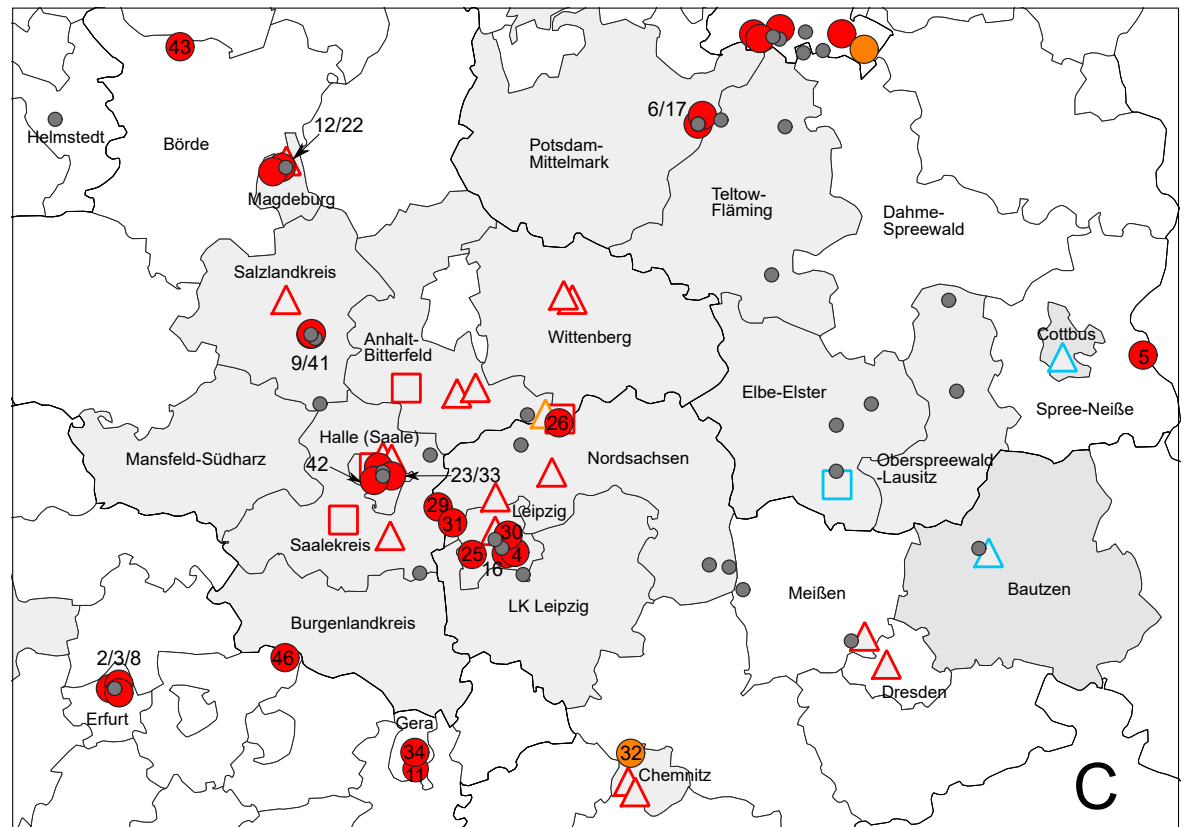
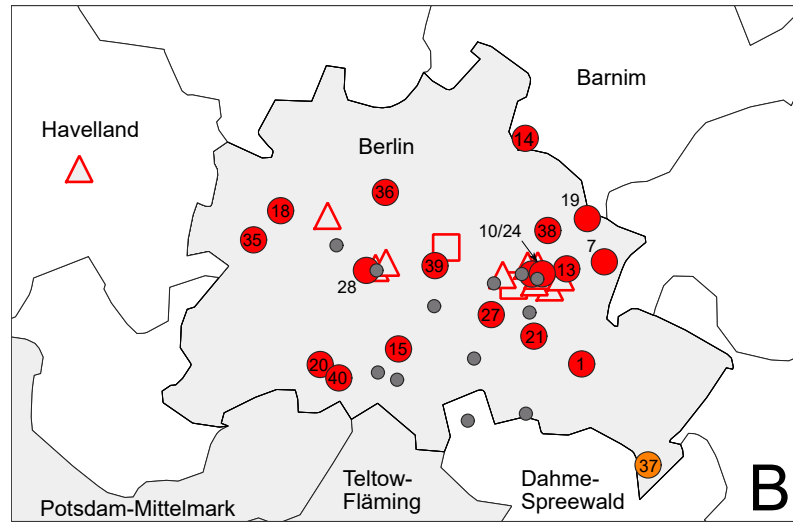
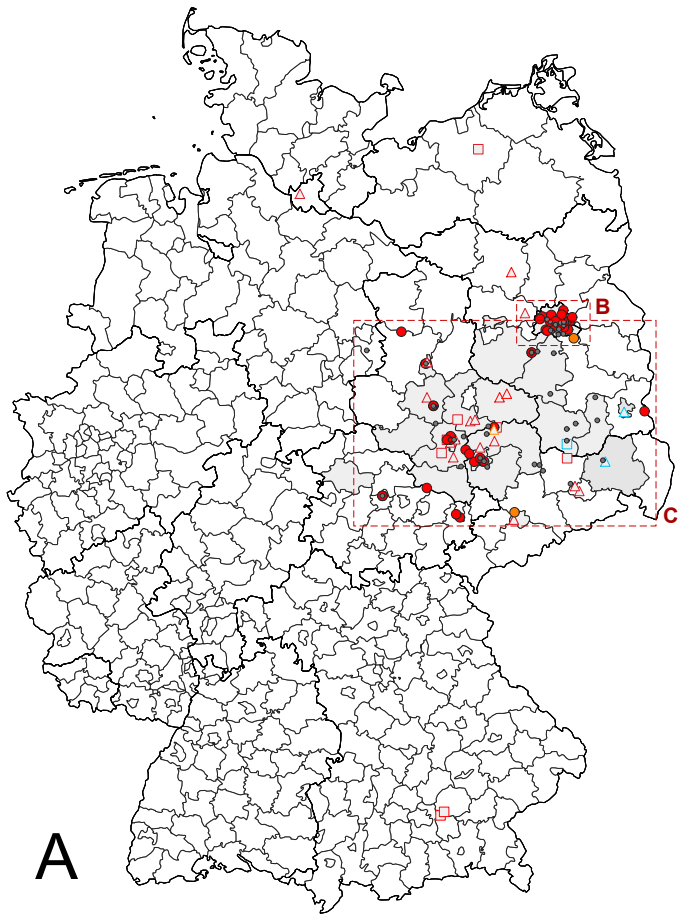
**WNV cases**

**Host (shape)**

- |                |  |
|----------------|--|
| ○ Captive bird |  Mosquito |
| △ Wild bird    |  Human    |
| □ Horse        |  |

**Clusters and subclusters (fill color)**

- |   |              |
|---|--------------|
|  | 2.5.3.2      |
|  | 2.5.3.4.3a   |
|  | 2.5.3.4.3c   |
|  | undetermined |



Grouping	WNV cases in the years		
	2018	2019	2020
2.5.3.2	ND	△	●
2.5.3.4.3a	□	△	ND
2.5.3.4.3c	□	△	●
Undetermined			●

## Supplementary material for

“An advanced sequence clustering and designation workflow reveals the enzootic maintenance of a dominant West Nile virus subclade in Germany”

Pauline Dianne Santos<sup>1,†</sup>, Anne Günther<sup>1,†</sup>, Markus Keller<sup>2</sup>, Timo Homeier-Bachmann<sup>3</sup>, Martin H. Groschup<sup>2,4</sup>, Martin Beer<sup>1</sup>, Dirk Höper<sup>1,†</sup>, Ute Ziegler<sup>2,4, †,\*</sup>

## Contents

- R-Code
- Figure S1
- Figure S1
- Table S1
- Table S2
- Table S3
- Table S4



## R-Code

```
### AP-Clustering of genome sequences based on an identity-matrix

## load necessary R-packages
library(apcluster)
library(writexl)

## prepare workspace
rm(list = ls()) # clean up workspace to prevent from interference between calculation and pre-existing data

## settings; when multiple values are provided, all possible combinations are tested
minStepNumbers <- c(1000, 2000, 5000, 10000) # the minimum number of steps to divide the input preference range for plateau calculations
stepFactor <- 10 # currently not used; Factor to calculate the allowed maximum step number from the used minStepNumbers
windowProportions <- c(0.01, 0.005, 0.0025, 0.001, 0.0001) # the fraction of the complete steps (see above) the partial dataset used for the APC should have
minPlateauWindows <- 3 # the allowed minimum the actual window may have (values < 3 do not make sense)
groupSizes <- c(5, 7, 10) # the minimum number of sequences of a subgroup to use as input for a further subgrouping
maxGroupDepth <- 5 # number of hierarchy levels to calculate with
1=Lineage/2=Clade/3=Subclade/4=Cluster/5=Subcluster

## load and prepare input data
setwd("M:/R-work/PS_wnv_apc/testWL2/") # choose the folder to read the input from and to save the output
dateipfad <- "M:/R-work/PS_wnv_apc/testWL2/WL2_R01_cleaned.csv" # choose the input file
sequencelidentityMatrix <- read.csv(dateipfad, row.names = 1) # read in the matrix of sequence identities

if(identical(colnames(sequencelidentityMatrix), rownames(sequencelidentityMatrix))) { # check whether or not the dimnames are identical, if not do not calculate because it might generate invalid results
  dissimilarityMatrix <- -1*((1-as.matrix(sequencelidentityMatrix))^2) # convert the sequence identity matrix into a matrix of dissimilarities as this is the input for affinity propagation clustering
  for(aktStepNumber in minStepNumbers) { # iterate the calculations over all preset numbers of steps over the input preference range
    for(winProp in windowProportions) { # iterate the calculations over all preset proportions for plateau definition
      for(aktGroupSize in groupSizes) { # iterate the calculations over all preset minimum group sizes
```

```
for(aktPlateauWindow in minPlateauWindows) {
  dateien <- list.files() # read in a list of files currently present in your target folder
  ## prepare necessary objects to accomodate results
  paramCollection <- data.frame(level = NA, group = NA, inputGroupSize = NA, usedStepWidth =
NA, setIterations = NA,
                                usedIterations = NA, minPrefRange = NA, maxPrefRange = NA,
terminatingInPref = NA,
                                defaultStepNumber = NA, lastStable = NA, longest = NA, defaultAPC = NA,
                                cutCrit = NA, usedWindowSize = NA) # set up a data.frame to collect all
relevant parameters used in the current iteration
  allResults <- vector("list", 4) # set up a list to collect all clustering results from the current
iteration
  names(allResults) <- c("group", "defaultAPResult", "cuttreeResult", "aggExResult") # name the
elements of the list

  ## calculate settings adjusted according to above input
  maxStepNumber <- aktStepNumber * stepFactor # currently not used; calculate the
maximum allowed step number
  initSteps <- (aktStepNumber + maxStepNumber) / 2 # currently not used; calculate the initial
number of steps to start with
  plateauWindow <- floor(aktStepNumber * winProp) # set the window size to fit the actual
step number and interrogate always the same portion of the overall range
  if(plateauWindow < aktPlateauWindow) plateauWindow <- aktPlateauWindow ## in case the
combined settings result in a window smaller than the minimum allowed window size, adjust the
setting to the allowed minimum

  ## prepare filenames to save results
  datensatz <- sub("\\.[:alpha:]]{1,}$", "", basename(dateipfad)) # extract the name of the
dataset from the filepath
  filename <- paste(datensatz, ".test.Affiliations-minSteps_", aktStepNumber, "-window_",
plateauWindow,
                    "-minMembers_", aktGroupSize, "-maxGroupDepth_", maxGroupDepth, ".xlsx", sep
= "") # construct filename containing the distinguishing parameters

  if(is.element(filename, dateien) == FALSE) { # check whether the calculation using the
recent parameter combination was already initiated; only if not, continue calculating, otherwise
skip to the next combination
    write_xlsx(data.frame("Analysis in progress"), filename, col_names = FALSE) # write a file
into the current folder to mark the parameter combination in progress
    print(paste("Analysis in progress: ", filename, sep = "")) # output user information

    seqSubset <- colnames(dissimilarityMatrix) # define the initial set of sequences, i.e. use
all sequences of the dataset
    affiliations <- data.frame(matrix(nrow = length(seqSubset), ncol = maxGroupDepth + 3)) #
set up an object to save the results of the APC; needs 3 more columns than the number of hierarchy
levels defined by maxGroupDepth
```

```
colnames(affiliations) <- c("accession", "affiliation", paste("affil", 0:maxGroupDepth, sep =
"0")) # set the column names

rownames(affiliations) <- colnames(dissimilarityMatrix) # set rownames identical with
colnames of the input identity matrix

affiliations$accession <- rownames(affiliations) # copy the rownames to the first column of
the result matrix

affiliations$affil00 <- 1 # set the initial affiliation level to 1 for all sequences

affiliations$affiliation <- 0 # set the affiliation 0 for all sequences

for(mgd in 0:(maxGroupDepth - 1)) { # iteratively run through the grouping for all
sequences for the given number of hierarchy levels

  prevLevel <- paste("affil", mgd, sep = "0") # the previous hierarchy level, the starting point
for subsetting the dataset

  currLevel <- paste("affil", (mgd + 1), sep = "0") # the current hierarchy level to be
determined for the respective subset of sequences

  affiliations[, currLevel] <- 0 # set the initial affiliations in the currently analysed hierarchy
level to the default value

  for(aktSubGroup in unique(affiliations$affiliation[affiliations[,prevLevel] > 0])) { # run the
grouping for the current hierarchy level for all subgroups of the preceding level

    seqSubset <- affiliations$accession[affiliations$affiliation == aktSubGroup] # generate
the list of sequence names belonging to the currently analysed subgroup

    if(length(seqSubset) < aktGroupSize) affiliations[seqSubset, currLevel] <- -1 else { #
check whether the number of sequences in the current group is sufficient according to the preset
minimum group size to allow for further subdivision; if not, set the current affiliation -1 to stop
further evaluation in the subsequent iterations

      workmat <- as.matrix(dissimilarityMatrix[seqSubset, seqSubset]) # if the current group
size allows for further subdivision, get the working matrix only containing data of the relevant
subset

      workmatAPC <- apcluster(workmat, details=TRUE, q=0.5) # calculate the AP-clustering
of the current data subset using the default input preference q

      prefRang <- preferenceRange(workmat, exact=TRUE) # determine the input preference
range of the data subset

      pStepWidth <- abs((prefRang[2] - prefRang[1]) / (aktStepNumber - 2)) # adjust the step
width to cover the complete input preference range in equal steps

      inPref <- unique(c(prefRang[1], seq(prefRang[1], prefRang[2], pStepWidth),
prefRang[2])) # calculate all input preferences to use in the APC iterations

      plateauWindow <- floor(length(inPref) * winProp) # set the window size to fit the
actual step number and interrogate always the same portion of the overall range

      if(plateauWindow < aktPlateauWindow) plateauWindow <- aktPlateauWindow # in case
the calculated window size for the determination of a cluster number plateau is lower than the
preset lower level, adjust the size of the window used to define the plateau to fit with the lower
limit

      if(length(inPref) > plateauWindow) { # test whether sufficient iterations are performed
to cover the set window for plateau determination, only start iterating if yes because otherwise an
error will occur

        clusTab <- data.frame(inPref, numClust = NA, windowStDev = NA, windowMean = NA,
increase = TRUE, stDevOK = TRUE) # prepare table to save the results of all clustering iterations to
enable testing whether or not the stopping criteria are met
```

```
i <- 0 # define counter
stopAPC <- FALSE # set the control variable
while(i < nrow(clusTab) & stopAPC == FALSE) { # repeat the calculations for AP
clustering of the current data subset until either of the stopping criteria is met
  i <- i + 1 # increase counter for current iteration
  j<-apcluster(workmat, p = clusTab$inPref[i]) # determine the number of AP clusters
in the data subset with the given input preference (as previously defined from the preference range
and chosen number of iterations)
  clusTab$numClust[i] <- length(j@clusters) # record the number of AP clusters
corresponding with the input preference
  if(i <= plateauWindow) { # check whether or not sufficient data for calculation of
mean and SD from number of clusters is available
    if(i == 1) clusTab>windowStDev[i] <- 0 else clusTab>windowStDev[i] <-
sd(clusTab$numClust[1:i]) # if not, set SD of cluster number within window 0 in case of first
iteration, otherwise adjust SD calculation to available data instead of preset window
    clusTab>windowMean[i] <- mean(clusTab$numClust[1:i]) # calculate mean from the
available data
  } else { # number of performed iterations higher than window size for plateau
definition
    clusTab>windowStDev[i] <- sd(clusTab$numClust[(i - plateauWindow + 1):i]) #
calculate SD of cluster number from recent and preceding iterations (in total preset number of
iterations)
    clusTab>windowMean[i] <- mean(clusTab$numClust[(i - plateauWindow + 1):i]) #
calculate mean cluster number from recent and preceding iterations (in total preset number of
iterations)
    clusTab$increase[i] <- clusTab>windowMean[i] >= clusTab>windowMean[(i-1)] # test
whether the number of clusters is the same as or larger than in the preceding iteration, because a
decrease is deemed a disruption and leads to termination of the iterative AP clustering
    tempTab <- clusTab[(i - plateauWindow + 1):i,] # make subset of the table only
containing data of the plateauWindow number of rows including the last iteration
    clusTab$stDevOK[i] <- nrow(tempTab[tempTab>windowStDev != 0,]) <
plateauWindow # test whether the SD of the cluster number returns to 0 after an increase of the
cluster number (this must be the case if the cluster number is stable for at least plateauWindow
iterations), if not a disruption occurred
    stopAPC <- !(clusTab$increase[i] == TRUE & clusTab$stDevOK[i] == TRUE) # check
whether or not both criteria to enter the next iteration, i.e. not to terminate the loop, are fulfilled
  }
}
setIterations <- nrow(clusTab) # record the set maximum number of iterations
clusTab <- clusTab[1:(i - plateauWindow),] # cut the table to the number of iterations
before the disruption occurred
usedIterations <- nrow(clusTab) # record the number of iterations with stable plateau
lastStable <- clusTab$numClust[nrow(clusTab)] # record the number clusters in the
last stable plateau
firstPlateau <- min(clusTab$numClust) # record the number of clusters in the first
observed plateau
plateauSummary <- clusTab$numClust # prepare the identification of the longest
plateau
```

```
plateauSummary <- plateauSummary[plateauSummary > firstPlateau] # only use
values higher than the first plateau (as per the definition in Susanne Fischer's paper the first plateau
is not valid)

plateauSummary <- summary(as.factor(plateauSummary), maxsum =
length(unique(plateauSummary))) # summarize how often each number of clusters was observed to
define the longest plateau, i.e. the number of clusters that was most often observed before the
disruption

if(is.element(TRUE, duplicated(plateauSummary))) longestPlateau <-
as.numeric(names(plateauSummary[plateauSummary == max(plateauSummary)])) else
longestPlateau <- as.numeric(names(which.max(plateauSummary))) # determine the number of
clusters constituting the longest plateau; in case 2 or more cluster numbers are present the same
number of iterations, use the higher number of clusters in order not to reduce the cluster number
too stringently

allPlateaus <- c(lastStable, longestPlateau) # concatenate the determined
clusternumbers from the longest and the last stable plateau

if(is.element(TRUE, allPlateaus < length(workmatAPC@clusters))) { # define the best
number of clusters to use and record the used choice; the best choice is the highest number of
clusters that is equal or lower than the number of clusters determined with the default input
preference, therefore, test whether either the last stable or the longest plateau are more stringent
than the default

  cutNum <- max(allPlateaus[allPlateaus < length(workmatAPC@clusters)]) # record
the number of clusters to use for cutting the tree (below)

  if(cutNum == lastStable) cutCrit <- "last" else cutCrit <- "longest" # record the choice
in case the default is replaced

} else { # the default value is used

  cutNum <- length(workmatAPC@clusters) # record the default value of the cluster
number to use it for tree cutting below

  cutCrit <- "defaultAPC" # record the used choice

}

aggdissimilarityMatrix <- aggExCluster(workmat, workmatAPC) # agglomerative
hierarchical clustering

grouping <- cutree(aggdissimilarityMatrix, k = cutNum) # cutting the tree to
determine the resulting grouping of sequences; k = number of groups to have = cluster number as
determined above

if(length(grouping@clusters) == 1) for(g in 1:length(grouping@clusters))
affiliations[rownames(workmat)[grouping@clusters[[g]]], currLevel] <- -3 else for(g in
1:length(grouping@clusters)) affiliations[rownames(workmat)[grouping@clusters[[g]]], currLevel] <-
g # record the grouping in the current subset of the current hierarchical level; in case the subset
cannot be further subdivided (number of clusters is 1), record -3 to label the grouping being
terminated for the subset because it cannot be further subdivided; in all other cases, record the
group affiliations per sequence

} else affiliations[seqSubset, currLevel] <- -2 # in case there is not enough steps for the
calculations, report -2 to label the subgroup for subsequent cycles and error analysis

}

## in the following lines, record all current settings of the iteration

paramCollection$terminatingInPref[nrow(paramCollection)] <-
clusTab$inPref[nrow(clusTab)]

paramCollection$level[nrow(paramCollection)] <- mgd
```

```
paramCollection$group[nrow(paramCollection)] <- aktSubGroup
paramCollection$inputGroupSize[nrow(paramCollection)] <- length(seqSubset)
paramCollection$usedStepWidth[nrow(paramCollection)] <- pStepWidth
paramCollection$setIterations[nrow(paramCollection)] <- setIterations
paramCollection$usedIterations[nrow(paramCollection)] <- usedIterations
paramCollection$minPrefRange[nrow(paramCollection)] <- prefRang[1]
paramCollection$maxPrefRange[nrow(paramCollection)] <- prefRang[2]
paramCollection$lastStable[nrow(paramCollection)] <- lastStable
if(length(longestPlateau > 0)) paramCollection$longest[nrow(paramCollection)] <-
longestPlateau else paramCollection$longest[nrow(paramCollection)] <- NA
paramCollection$defaultAPC[nrow(paramCollection)] <- length(workmatAPC@clusters)
paramCollection$cutCrit[nrow(paramCollection)] <- cutCrit
paramCollection$usedWindowSize[nrow(paramCollection)] <- plateauWindow
paramCollection <- rbind(paramCollection, NA) # add the next line to the table to
accommodate the data of the next iteration
## End parameter recording

## in the following lines, record all results of the current iteration
allResults$group <- append(allResults$group, aktSubGroup)
allResults$defaultAPresult <- append(allResults$defaultAPresult, workmatAPC)
allResults$aggExResult <- append(allResults$aggExResult, aggdisimilarityMatrix)
allResults$cuttreeResult <- append(allResults$cuttreeResult, grouping)
## End results recording
}

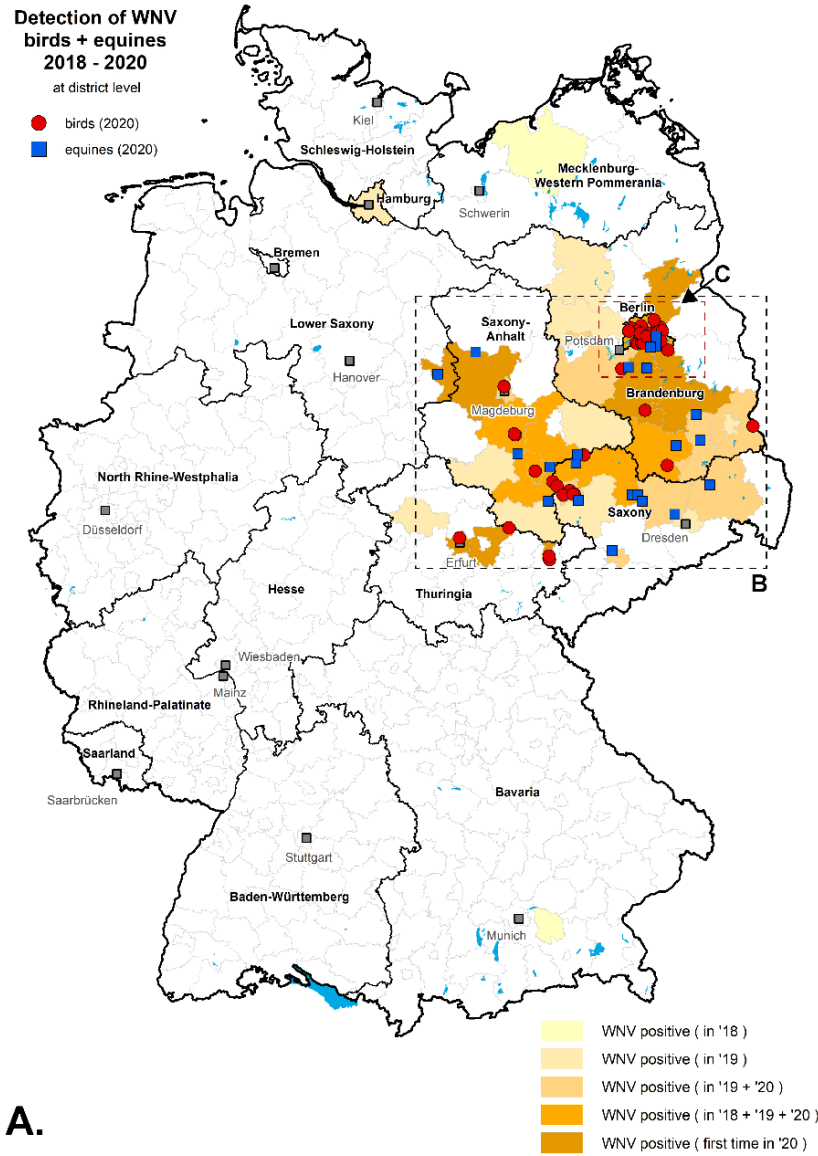
if(mgd == 0) affiliations$affiliation[affiliations[, currLevel] > 0] <- affiliations[affiliations[,
currLevel] > 0, currLevel] else affiliations$affiliation[affiliations[, currLevel] > 0] <-
paste(affiliations$affiliation[affiliations[, currLevel] > 0], affiliations[affiliations[, currLevel] > 0,
currLevel], sep = ".") # construct the overall group designation from the previously present portion
and the currently analyzed hierarchy level; in case it is the first level iteration, replace the present
values with the current
}
affiliations$affil00 <- NULL # delete the initial grouping

## save results to disk
write_xlsx(affiliations, filename)
write_xlsx(paramCollection, sub("Affiliations", "usedParameters", filename))
save.image(file = sub("Affiliations", "CompleteData", sub("xlsx", "RData", filename)))
}
}
}
}
}
} else print("Please check the column and row names in your input file! They must be identical!")
```

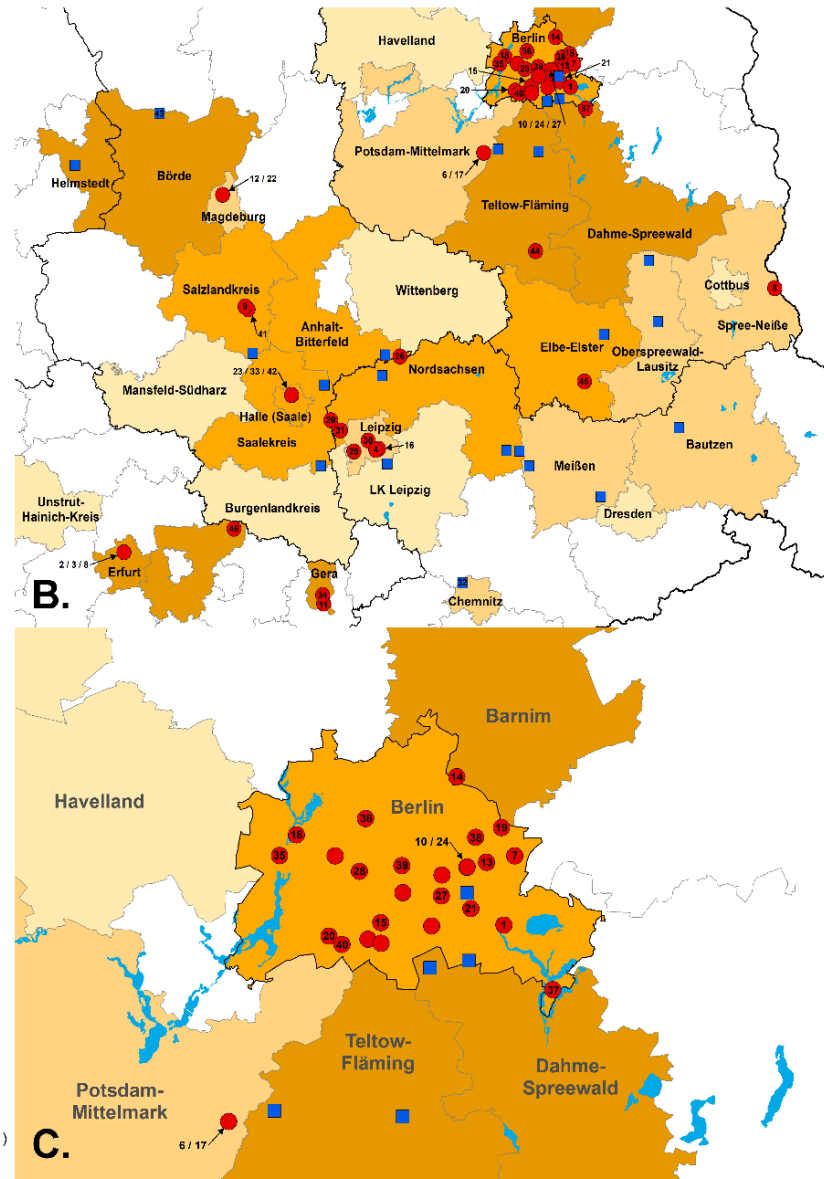
**Figure S1.** Geographic distribution of WNV cases in Germany in 2020 (depicted on district level) as shown in A. Specific areas with WNV cases in the areas of Saxony, Saxony-Anhalt, Thuringia, Berlin and Brandenburg were shown in B and WNV cases in Berlin and surrounding areas in Brandenburg were shown in C. Blue squares and red circles indicate notifiable WNV cases of horses and birds. WNV cases with numbers indicated that these samples were subjected to whole-genome sequencing. WNV cases that were not selected for sequencing (e.g., IgM-positive cases or high  $C_q$  values) remain unnumbered. Intensity of the colored background at district level indicates the frequency, how often an area was affected by WNV activity in prior years.

**Detection of WNV  
birds + equines  
2018 - 2020**  
at district level

- birds (2020)
- equines (2020)



**A.**

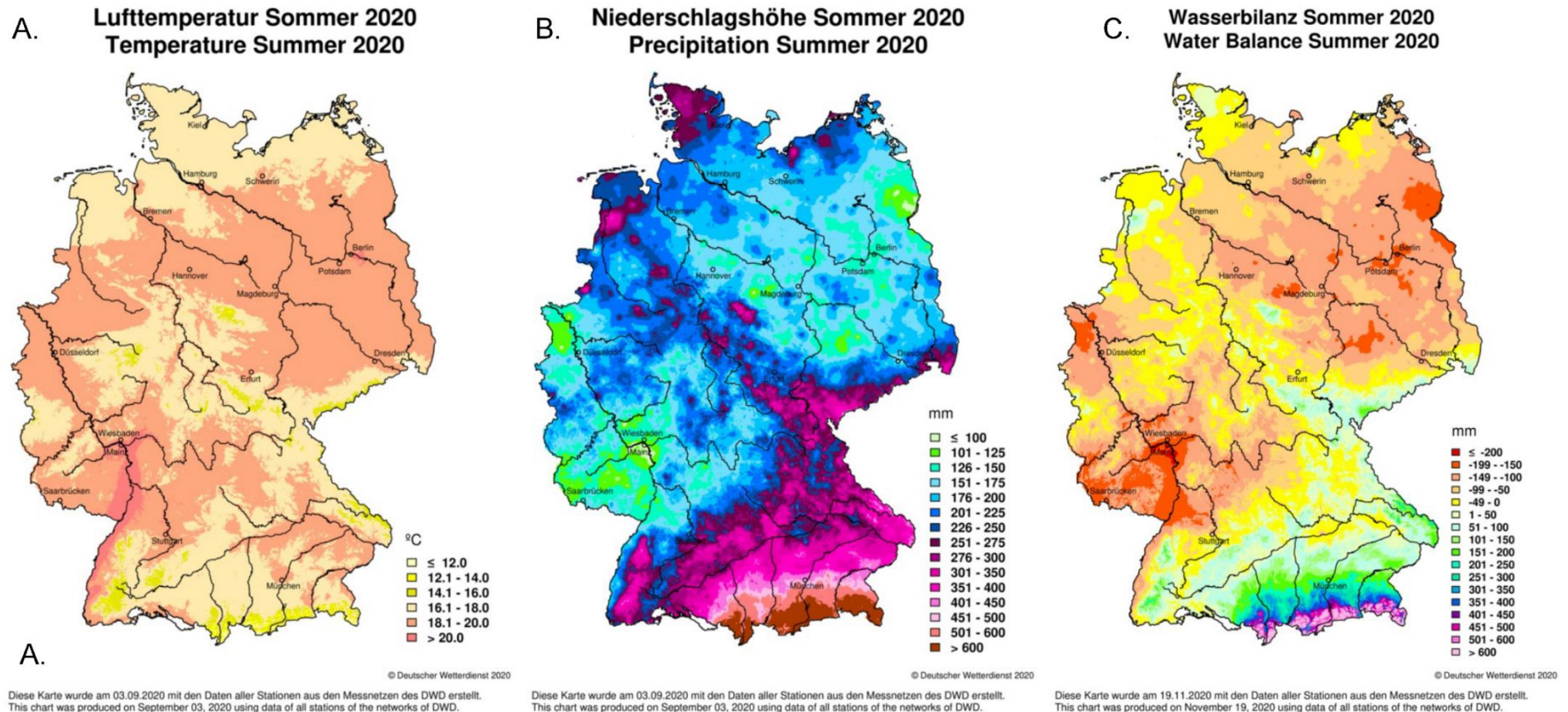


**B.**

**C.**



**Figure S2** Climatological maps of Germany displaying A) temperature (in degree celsius), B) precipitation (in millimeter) and C) water balance (in millimeter) based on data collected in summer 2020. Climatological maps were downloaded from Deutscher Wetterdienst; [https://www.dwd.de/EN/climate\\_environment/climatemonitoring/germany/germany\\_node.html](https://www.dwd.de/EN/climate_environment/climatemonitoring/germany/germany_node.html) (Deutscher Wetterdienst 2020)



Deutscher Wetterdienst (2021), 'Climatological maps of Germany',  
<<https://www.dwd.de/EN/ourservices/klimakartendeutschland/klimakartendeutschland.html?nn=495490>>, accessed 15.07.2021.

**Table S1** West Nile Virus primer sequences from Sikkema et al. 2020. Each primer stock was normalized to 100 micromolar concentration. Volumes of each primer per primer mix (mix 1 or 2) were specified in the table below. These primers mixes were then subjected to 1:10 dilution.

Primer number	Mix	Primer	Primer sequence	Used volume (μl)
1	1	WNVUS1_1_LEFT	GCCTGTGTGARCTGACAACTTAG	10
2	1	WNVUS1_1_RIGHT	CTTTCTTTTGTGTTTGRGCTCCG	10
3	1	WNVUS1_3_LEFT	AGTTACCCTCTCTAACTCCAAG	15
4	1	WNVUS1_3_LEFT_2	GTGACCCTCTCCAACCTCCAGG	15
5	1	WNVUS1_3_RIGHT	CARGAAGTCTCTGTTRCTCATTCC	15
6	1	WNVUS1_5_LEFT_2	GTGTCCAACCATGGGTGAAGCC	10
7	1	WNVUS1_5_LEFT	GCCCGACCATGGGAGAAGCT	10
8	1	WNVUS1_5_RIGHT_2	GTGGCATGAGGTTCTCAAACCTCC	10
9	1	WNVUS1_5_RIGHT	GGCGTGTGGTTCCTCAAACCTCC	10
10	1	WNVUS1_7_LEFT_2	TCTGAAGTGTAGGGTGAAGATGGAG	10
11	1	WNVUS1_7_LEFT	GTCATTTGAAGTGTAGAGTGAAGATGG	10
12	1	WNVUS1_7_RIGHT	GAGGTGAAMACCCCTCCAACCTG	10
13	1	WNVUS1_9_LEFT	GTGGATGGGMATCAATGCYCGT	10
14	1	WNVUS1_9_RIGHT_2	CTCTTGCCCCAAGCCTTCCAAC	10
15	1	WNVUS1_9_RIGHT	CTTCCCCAGGCCTTCCAGC	10
16	1	WNVUS1_11_LEFT	CACAACKGAATGYGACTCGAAGAT	10
17	1	WNVUS1_11_RIGHT	ACGGTGTCCGCAGCTCTCAC	10
18	1	WNVUS1_11_RIGHT_2	CACGGTGTCCGCAACTRTCAC	10
19	1	WNVUS1_13_LEFT_2	GGCAGCAGGAAAAGACCCTCGTGC	10
20	1	WNVUS1_13_LEFT	GACATGATGAAAAGACCCTCGTGC	10
21	1	WNVUS1_13_RIGHT_2	CTCTGGTTGGTCCACCTTGC	10
22	1	WNVUS1_13_RIGHT	CTCCTGGTTGGTCCATCTCGC	10
23	1	WNVUS1_15_LEFT_2	CAAATGTGGTGGTGCCGCTGC	10
24	1	WNVUS1_15_LEFT	CGACATCAAACGTGGTTGTTCCG	10
25	1	WNVUS1_15_RIGHT_2	CYGTCTCTCAATCCACATGTC	10
26	1	WNVUS1_15_RIGHT	CGCCGTTCTCTCAATCCACATATC	10
27	1	WNVUS1_17_LEFT_2	ATAAGTGCCTACACACCYTGGGC	10
28	1	WNVUS1_17_LEFT	GGAARATATGGATGCTCAGAATGG	10
29	1	WNVUS1_17_RIGHT_2	CCCCAATTTCTCCTTCTGGTGTGTC	10
30	1	WNVUS1_17_RIGHT	TTTGAACACCCCTGGTTTCGTC	10
31	1	WNVUS1_19_LEFT_2	CCATTGTGCAAGGAGAGAGAATGG	10
32	1	WNVUS1_19_LEFT	CGGATTGCAACCTGAGATGCTG	10
33	1	WNVUS1_19_RIGHT_2	CGATGCTCGCTGGATCCGTG	10
34	1	WNVUS1_19_RIGHT	CATGAATATTGCCGCCGCTC	10
35	1	WNVUS1_21_LEFT_2	GGAAAGACCGTTTGGTTTGTTC	10
36	1	WNVUS1_21_LEFT	GGGAAGACGGTTTGGTTTGTGC	10
37	1	WNVUS1_21_RIGHT_2	GAGTCGTCTTCATTCGTGTGCC	10
38	1	WNVUS1_21_RIGHT	GTTGGAATCATCTCATTGTGTGC	10
39	1	WNVUS1_23_LEFT	CGGCTGGAGTGCATACCACG	10
40	1	WNVUS1_23_LEFT_2	CAGCAGGAATATCATACCATGACC	10
41	1	WNVUS1_23_RIGHT_2	CTATTGTCTGAAGGGCGTCCGG	10

Primer number	Mix	Primer	Primer sequence	Used volume (μl)
42	1	WNVUS1_23_RIGHT	GAATACTCCCATGGTCATCACACTC	10
43	1	WNVUS1_25_LEFT_2	CAGGAACGAAAATAGCAGGCATGC	10
44	1	WNVUS1_25_LEFT	GGAACGAAGATCGCCGGAATG	10
45	1	WNVUS1_25_RIGHT_2	GCTTCCGCTTGCCAGCCTG	10
46	1	WNVUS1_25_RIGHT	GCTGAGCGCATTGCCTCAGC	10
47	1	WNVUS1_27_LEFT_2	CAGTCATGCAGAAAAARGTTGGACAG	10
48	1	WNVUS1_27_LEFT	GATCTTGGTGTCTCTAGCTGCAG	10
49	1	WNVUS1_27_RIGHT_2	CGAGATCCACAACCTTTCCAC	10
50	1	WNVUS1_27_RIGHT	CATCCAAGGTCAATCACTTTTCCG	10
51	1	WNVUS1_29_LEFT_2	CTGGCCATGAAGAGCCACAAC	10
52	1	WNVUS1_29_LEFT	GTACAGGAAGTGAAAGGGTACACG	10
53	1	WNVUS1_29_RIGHT_2	GTTGACATCTTCTCAAAGTGGGG	10
54	1	WNVUS1_29_RIGHT	GCCCTGGTTCCTTCCCAAG	10
55	1	WNVUS1_31_LEFT_2	GAATACAGCTCCACATGGCACC	10
56	1	WNVUS1_31_LEFT	GAGAACCACCCATATAGAACCTGG	10
57	1	WNVUS1_31_RIGHT	CTCTTCCCATCATGTTGTARATGC	10
58	1	WNVUS1_33_LEFT_2	GGGTACATCTTGAAGGAAGTYGG	10
59	1	WNVUS1_33_LEFT	GTTACATCCTGCGTGAAGTTGGC	10
60	1	WNVUS1_33_RIGHT	CSCATTCTCAAACAGCCAGG	10
61	1	WNVUS1_35_LEFT_2	GGTGGTATGACTGGCAGCAGG	10
62	1	WNVUS1_35_LEFT	GATGGTATGATTGGCAGCAGGTTC	10
63	1	WNVUS1_35_RIGHT	GTCTTCCATCCAYCATTCTCCTC	10
64	1	WNVUS1_37_LEFT	GAGAAGTATGYGGATTACATGAGYTC	15
65	1	WNVUS1_37_RIGHT	GGTCTCCTCTAACCTCTAGTCC	15
66	2	WNVUS1_2_RIGHT_2	CGGGCTGTCAATATGCTAAAACGC	10
67	2	WNVUS1_2_RIGHT	GTGCACCAGCAGTCAATGTCTTC	10
68	2	WNVUS1_2_LEFT	GTGCACCAACAGTCGATGTCTTC	10
69	2	WNVUS1_4_LEFT	GGATGCTAGGAAGCAACACAATGC	10
70	2	WNVUS1_4_RIGHT_2	GATGCTTGGRAGCAACACCATG	10
71	2	WNVUS1_4_RIGHT	TGCTYCCCTTTCCAAACAGTCC	10
72	2	WNVUS1_4_LEFT_2	GCTTCCTTTGCCAAATAGTCCGC	10
73	2	WNVUS1_6_LEFT	GACTGTGARCCACGGTCAGG	10
74	2	WNVUS1_6_RIGHT_2	CCGGTGTATTGCAGTTCCAACAC	10
75	2	WNVUS1_6_RIGHT	GCAATTCCAACACCACAGTGCC	10
76	2	WNVUS1_8_LEFT_2	GTGAATCCATTTGTGTCTGTGGCC	10
77	2	WNVUS1_8_LEFT	GTCAACCCTTTTGTTCAGTGGCC	10
78	2	WNVUS1_8_RIGHT_2	GATCCATCCAGGCTTCCACATC	10
79	2	WNVUS1_8_RIGHT	GGTCCATCCAAGCCTCCACATC	10
80	2	WNVUS1_10_LEFT_2	AGACTCGAGCACCAAATGTGGG	10
81	2	WNVUS1_10_LEFT	CCAGACTGGAGCATCAAATGTGG	10
82	2	WNVUS1_10_RIGHT	GAACYGCCCTYTCAAGCTTCC	10
83	2	WNVUS1_12_LEFT	GAAGTYAAATCATGYACSTGGCC	10
84	2	WNVUS1_12_RIGHT	CTTGCGAAGGACCTCCTGGG	10
85	2	WNVUS1_14_LEFT_2	GTCCTAGTGTGGGGGTATTACG	10
86	2	WNVUS1_14_LEFT	CCTGGTGTGGGGGCATTAC	10
87	2	WNVUS1_14_RIGHT_2	GCAGATGAGGCAAGCYCCTTTC	10

Primer number	Mix	Primer	Primer sequence	Used volume (μl)
88	2	WNVUS1_14_RIGHT	CAAGCATARCAGACTTGCTCCTTTC	10
89	2	WNVUS1_16_LEFT_2	CTGCAGTTGGACTIONCATGTTTGCC	10
90	2	WNVUS1_16_LEFT	GCTGTCGGCYTRATGTTTGCCA	10
91	2	WNVUS1_16_RIGHT_2	GGTGATGGTGTGTCCCAAAGRAC	10
92	2	WNVUS1_16_RIGHT	GAGGGAGTGTCCACARCAC	10
93	2	WNVUS1_18_LEFT_2	CCACACACTATGGCACACCAC	10
94	2	WNVUS1_18_LEFT	GCAGGAGCRGGCGTGATG	10
95	2	WNVUS1_18_RIGHT_2	CTCARTCTTTTGTGATGGCCTCC	10
96	2	WNVUS1_18_RIGHT	GCCACAGATCATCAAAGAGGCC	10
97	2	WNVUS1_20_LEFT_2	GATGTCTCCACACAGAGTCCC	10
98	2	WNVUS1_20_LEFT	GATGTCTCCTCACAGGGTGCC	10
99	2	WNVUS1_20_RIGHT_2	GAAAGTCGTAYGAGACGGAGTAC	10
100	2	WNVUS1_20_RIGHT	GGGTACTIONTGTCTCATAGGACTTTC	10
101	2	WNVUS1_22_LEFT_2	GCTCAGCGGAGAGGACGC	10
102	2	WNVUS1_22_LEFT	CGCCCAGAGACGTGGACG	10
103	2	WNVUS1_22_RIGHT_2	CTTCTCTCACCCACTIONTCGTG	10
104	2	WNVUS1_22_RIGHT	GGCCTCAGAATCTTCCTTTCACC	10
105	2	WNVUS1_24_LEFT_2	GATCACAAATCGGGCTCGTTGAG	10
106	2	WNVUS1_24_LEFT	CGTTCTCAGATAGGGCTCATTGAG	10
107	2	WNVUS1_24_RIGHT_2	CAACTCCCAGRGTCTGTCTCTC	10
108	2	WNVUS1_24_RIGHT	CTCCTTGACCTCAATTCTTTGCC	10
109	2	WNVUS1_26_LEFT_2	GTGGACGTTGGTGTGTCAGCTC	10
110	2	WNVUS1_26_LEFT	CTTCGTGATGTTGGAGTGTGCG	10
111	2	WNVUS1_26_RIGHT_2	GTTGCATTCCACACTGAACTAGC	10
112	2	WNVUS1_26_RIGHT	CCAAACAGAGCTTGCTCCATTCTC	10
113	2	WNVUS1_28_LEFT_2	GGGAAGTTTGAAGGAGAGACTC	10
114	2	WNVUS1_28_LEFT	GTACCGCAAAGAGGCCATCATC	10
115	2	WNVUS1_28_RIGHT_2	CCAATGTCACAGAGCAGTGTGTC	10
116	2	WNVUS1_28_RIGHT	GARGACTCTCCGATGTCACAAAG	10
117	2	WNVUS1_30_LEFT_2	CCATGAGATGTACTGGGTGAGY	15
118	2	WNVUS1_30_LEFT	GACTGGTCAGAAACCCACTCTC	15
119	2	WNVUS1_30_RIGHT_2	GAAGGGAGTAGTGTGATCATGG	15
120	2	WNVUS1_30_RIGHT	CATIONCTGTTGACCGAAAGGAG	15
121	2	WNVUS1_32_LEFT_2	GGAAGAACGCCCCGGAAGC	10
122	2	WNVUS1_32_LEFT	GAGGAGCGCCAGAGARGCAG	10
123	2	WNVUS1_32_RIGHT_2	CAGCAGTTCAAGAACCTTCGCTTC	10
124	2	WNVUS1_32_RIGHT	CCAAGTCAGCTCTCGTGATGCG	10
125	2	WNVUS1_34_LEFT_2	GTGAAAGTGATGCGCCCGGC	10
126	2	WNVUS1_34_LEFT	GTCGTGAAAGTGATGAGGCCAG	10
127	2	WNVUS1_34_RIGHT_2	GAGAWATGCGAGCTCTGCCTAC	10
128	2	WNVUS1_34_RIGHT	CGCACATTCCATCCAGCCCC	10
129	2	WNVUS1_36_LEFT_2	CGCAAAGGAGAATGGATGACGAC	10
130	2	WNVUS1_36_LEFT	CCATGCAGGAGGAGAGTGGATG	10
131	2	WNVUS1_36_RIGHT	CGTCTACTCAACTIONTCCGGTGG	10
132	2	WNVUS1_38_LEFT	CCCTCAGAACCGTCTCGGAAG	10
133	2	WNVUS1_38_RIGHT	GCACTIONTGCCGTGTGGCTG	10

**Table S2** Samples used to validate the WNV multiplex PCR High-throughput sequencing (HTS) in comparison with the result of unbiased and direct HTS approach.

Sample			Reference sequence				This study			Result of sequence comparison
Code	ID	Cq value	Library ID	applied protocol	INSDC Accesssion	Length (nt)	Library ID	INSDC Accesssion	Length (nt)	
C1	ED-I-62/19	22.9	lib03378	Wylezich et al 2018	LR743425	11,060	lib04562	XX	10,989	identical
C2	ED-I-156/19	11.8	lib03418	Wylezich et al 2018	LR743423	11,027	lib04563	XX	10,989	Identical
C3	ED-I-155/19	17.5	lib03420	Wylezich et al 2018	LR743422	11,010	lib04564	XX	10,987	Identical
C4	ED-I-115/19	31.5	lib03988	Wylezich et al 2021	LR989891	6,470	lib04565	XX	10,989	8 substitutions <sup>1</sup>
C5	ED-I-127-18	29.4	lib03224	Wylezich et al 2021	Unpublished	6,786	lib04748	XX	10,988	2 substitutions <sup>1</sup>

<sup>1</sup> based on available partial reference sequence; insertions and deletions not considered

**Table S3** List of full genome sequences retrieved from Genbank

Accession number	Used in Dataset
DQ116961	WL2
HQ537483	WL2
JN858070	WL2
KC407673	WL2
KC496015	WL2
KC496016	WL2
KF179639	WL2
KF179640	WL2
KF588365	WL2
KF647249	WL2
KF647250	WL2
KF647251	WL2
KF647252	WL2
KF823806	WL2
KJ577738	WL2
KJ577739	WL2
KJ883342	WL2
KJ883343	WL2
KJ883344	WL2
KJ883345	WL2
KJ883346	WL2
KJ883348	WL2
KJ883349	WL2
KJ883350	WL2
KM203860	WL2
KM203861	WL2
KM203862	WL2
KM203863	WL2
KM659876	WL2
KP109691	WL2
KP109692	WL2
KP780837	WL2
KP780838	WL2
KP780839	WL2
KP789953	WL2
KP789954	WL2
KP789955	WL2
KP789956	WL2
KP789957	WL2
KP789958	WL2
KP789959	WL2
KP789960	WL2
KT207792	WL2
KT359349	WL2
KT757318	WL2

Accession number	Used in Dataset
KT757319	WL2
KT757320	WL2
KT757321	WL2
KT757322	WL2
KT757323	WL2
KU206781	WL2
KU573080	WL2
KU573081	WL2
KU573082	WL2
KU573083	WL2
KX375812	WL2
KY594040	WL2
LR743421	WL2
LR743422	WL2
LR743423	WL2
LR743424	WL2
LR743425	WL2
LR743426	WL2
LR743427	WL2
LR743428	WL2
LR743429	WL2
LR743430	WL2
LR743431	WL2
LR743432	WL2
LR743433	WL2
LR743434	WL2
LR743435	WL2
LR743436	WL2
LR743437	WL2
LR743442	WL2
LR743443	WL2
LR743444	WL2
LR743445	WL2
LR743446	WL2
LR743447	WL2
LR743448	WL2
LR743449	WL2
LR743450	WL2
LR743451	WL2
LR743452	WL2
LR743453	WL2
LR743454	WL2
LR743455	WL2
LR743456	WL2
LR743457	WL2
LR743458	WL2

Accession number	Used in Dataset
LR989885	WL2
LR989888	WL2
MF984337	WL2
MF984338	WL2
MF984339	WL2
MF984340	WL2
MF984341	WL2
MF984342	WL2
MF984343	WL2
MF984344	WL2
MF984345	WL2
MF984346	WL2
MF984347	WL2
MF984348	WL2
MF984349	WL2
MF984350	WL2
MF984351	WL2
MF984352	WL2
MH021189	WL2
MH244510	WL2
MH244511	WL2
MH244512	WL2
MH244513	WL2
MH549209	WL2
MH910045	WL2
MH924836	WL2
MH986055	WL2
MH986056	WL2
MK473443	WL2
MK947396	WL2
MK947397	WL2
MN480792	WL2
MN480793	WL2
MN480794	WL2
MN480795	WL2
MN481589	WL2
MN481590	WL2
MN481591	WL2
MN481592	WL2
MN481593	WL2
MN481594	WL2
MN481595	WL2
MN481596	WL2
MN481597	WL2
MN652878	WL2
MN652879	WL2



Accession number	Used in Dataset
MN652880	WL2
MN794935	WL2
MN794937	WL2
MN794938	WL2
MN794939	WL2
MN939557	WL2
MN939558	WL2
MN939559	WL2
MN939560	WL2
MN939561	WL2
MN939562	WL2
MN939562	WL2
MN939564	WL2
MT341470	WL2
MT341471	WL2
MT341472	WL2
MT863560	WL2
MT863561	WL2
MW036634	WL2
MW142223	WL2
MW142224	WL2
MW142226	WL2
MW142227	WL2
AF196835	TD01 / TD03
AY277251	TD01 / TD03
AY532665	TD01 / TD03
AY701412	TD01 / TD03
AY701413	TD01 / TD03
AY765264	TD01 / TD03
DQ176636	TD01 / TD03
DQ256376	TD01 / TD03
DQ786573	TD01 / TD03
EF429197	TD01 / TD03
EF429198	TD01 / TD03
EF429199	TD01 / TD03
EF429200	TD01 / TD03
EU082200	TD01 / TD03
EU249803	TD01 / TD03
FJ159129	TD01 / TD03
FJ159130	TD01 / TD03
FJ159131	TD01 / TD03
FJ425721	TD01 / TD03
FJ483548	TD01 / TD03
FJ483549	TD01 / TD03
FJ766331	TD01 / TD03
FJ766332	TD01 / TD03

<b>Accession number</b>	<b>Used in Dataset</b>
GQ379161	TD01 / TD03
GQ851602	TD01 / TD03
GQ851603	TD01 / TD03
GQ851604	TD01 / TD03
GQ851605	TD01 / TD03
GQ851606	TD01 / TD03
GQ851607	TD01 / TD03
GQ903680	TD01 / TD03
GU011992	TD01 / TD03
HM051416	TD01 / TD03
HM147822	TD01 / TD03
HM147823	TD01 / TD03
HM147824	TD01 / TD03
HM152775	TD01 / TD03
HQ537483	TD01 / TD03
JF707789	TD01 / TD03
JF719066	TD01 / TD03
JF719067	TD01 / TD03
JF719068	TD01 / TD03
JF719069	TD01 / TD03
JN393308	TD01 / TD03
JN858069	TD01 / TD03
JN858070	TD01 / TD03
JQ928174	TD01 / TD03
JQ928175	TD01 / TD03
JX041628	TD01 / TD03
JX041629	TD01 / TD03
JX041630	TD01 / TD03
JX041632	TD01 / TD03
JX041634	TD01 / TD03
JX123030	TD01 / TD03
JX123031	TD01 / TD03
JX442279	TD01 / TD03
JX556213	TD01 / TD03
KC407673	TD01 / TD03
KC496015	TD01 / TD03
KC496016	TD01 / TD03
KC601756	TD01 / TD03
KC954092	TD01 / TD03
KF179639	TD01 / TD03
KF179640	TD01 / TD03
KF234080	TD01 / TD03
KF647251	TD01 / TD03
KF647253	TD01 / TD03
KJ831223	TD01 / TD03
KJ883346	TD01 / TD03

<b>Accession number</b>	<b>Used in Dataset</b>
KJ934710	TD01 / TD03
KM052152	TD01 / TD03
KM203861	TD01 / TD03
KM203862	TD01 / TD03
KM203863	TD01 / TD03
KP109692	TD01 / TD03
KP780837	TD01 / TD03
KP780838	TD01 / TD03
KP780839	TD01 / TD03
KP780840	TD01 / TD03
KT163243	TD01 / TD03
KT207791	TD01 / TD03
KT207792	TD01 / TD03
KT359349	TD01 / TD03
KT934796	TD01 / TD03
KT934797	TD01 / TD03
KT934798	TD01 / TD03
KT934799	TD01 / TD03
KT934800	TD01 / TD03
KT934801	TD01 / TD03
KT934802	TD01 / TD03
KT934803	TD01 / TD03
KU588135	TD01 / TD03
KY703854	TD01 / TD03
KY703855	TD01 / TD03
KY703856	TD01 / TD03
AF196835	TD02 / TD03
AF202541	TD02 / TD03
AF206518	TD02 / TD03
AF260967	TD02 / TD03
AF260968	TD02 / TD03
AF260969	TD02 / TD03
AF317203	TD02 / TD03
AF404753	TD02 / TD03
AF404754	TD02 / TD03
AF404755	TD02 / TD03
AF404756	TD02 / TD03
AF404757	TD02 / TD03
AF481864	TD02 / TD03
AF533540	TD02 / TD03
AJ965626	TD02 / TD03
AJ965628	TD02 / TD03
AM404308	TD02 / TD03
AY262283	TD02 / TD03
AY268132	TD02 / TD03
AY268133	TD02 / TD03

<b>Accession number</b>	<b>Used in Dataset</b>
AY274504	TD02 / TD03
AY277252	TD02 / TD03
AY278441	TD02 / TD03
AY278442	TD02 / TD03
AY289214	TD02 / TD03
AY603654	TD02 / TD03
AY646354	TD02 / TD03
AY660002	TD02 / TD03
AY701412	TD02 / TD03
AY701413	TD02 / TD03
AY712945	TD02 / TD03
AY712946	TD02 / TD03
AY712947	TD02 / TD03
AY712948	TD02 / TD03
AY795965	TD02 / TD03
DQ005530	TD02 / TD03
DQ080051	TD02 / TD03
DQ080052	TD02 / TD03
DQ080053	TD02 / TD03
DQ080054	TD02 / TD03
DQ080055	TD02 / TD03
DQ080056	TD02 / TD03
DQ080057	TD02 / TD03
DQ080058	TD02 / TD03
DQ080059	TD02 / TD03
DQ080060	TD02 / TD03
DQ080061	TD02 / TD03
DQ080062	TD02 / TD03
DQ080063	TD02 / TD03
DQ080064	TD02 / TD03
DQ080065	TD02 / TD03
DQ080066	TD02 / TD03
DQ080067	TD02 / TD03
DQ080068	TD02 / TD03
DQ080069	TD02 / TD03
DQ080070	TD02 / TD03
DQ080071	TD02 / TD03
DQ080072	TD02 / TD03
DQ118127	TD02 / TD03
DQ164186	TD02 / TD03
DQ164187	TD02 / TD03
DQ164188	TD02 / TD03
DQ164189	TD02 / TD03
DQ164190	TD02 / TD03
DQ164191	TD02 / TD03
DQ164192	TD02 / TD03

<b>Accession number</b>	<b>Used in Dataset</b>
DQ164193	TD02 / TD03
DQ164194	TD02 / TD03
DQ164195	TD02 / TD03
DQ164196	TD02 / TD03
DQ164197	TD02 / TD03
DQ164198	TD02 / TD03
DQ164199	TD02 / TD03
DQ164200	TD02 / TD03
DQ164201	TD02 / TD03
DQ164202	TD02 / TD03
DQ164203	TD02 / TD03
DQ164204	TD02 / TD03
DQ164205	TD02 / TD03
DQ164206	TD02 / TD03
DQ176637	TD02 / TD03
DQ211652	TD02 / TD03
DQ256376	TD02 / TD03
DQ374650	TD02 / TD03
DQ374651	TD02 / TD03
DQ374652	TD02 / TD03
DQ374653	TD02 / TD03
DQ377178	TD02 / TD03
DQ377179	TD02 / TD03
DQ377180	TD02 / TD03
DQ411029	TD02 / TD03
DQ411030	TD02 / TD03
DQ411031	TD02 / TD03
DQ411032	TD02 / TD03
DQ411033	TD02 / TD03
DQ411034	TD02 / TD03
DQ411035	TD02 / TD03
DQ431693	TD02 / TD03
DQ431694	TD02 / TD03
DQ431695	TD02 / TD03
DQ431696	TD02 / TD03
DQ431697	TD02 / TD03
DQ431698	TD02 / TD03
DQ431699	TD02 / TD03
DQ431700	TD02 / TD03
DQ431701	TD02 / TD03
DQ431702	TD02 / TD03
DQ431703	TD02 / TD03
DQ431704	TD02 / TD03
DQ431705	TD02 / TD03
DQ431706	TD02 / TD03
DQ431707	TD02 / TD03

<b>Accession number</b>	<b>Used in Dataset</b>
DQ431708	TD02 / TD03
DQ431709	TD02 / TD03
DQ431710	TD02 / TD03
DQ431711	TD02 / TD03
DQ431712	TD02 / TD03
DQ666448	TD02 / TD03
DQ666449	TD02 / TD03
DQ666450	TD02 / TD03
DQ666451	TD02 / TD03
DQ666452	TD02 / TD03
DQ786572	TD02 / TD03
DQ786573	TD02 / TD03
EU249803	TD02 / TD03
FJ483548	TD02 / TD03
FJ483549	TD02 / TD03
FJ527738	TD02 / TD03
FJ766331	TD02 / TD03
FJ766332	TD02 / TD03
GQ379157	TD02 / TD03
GQ379158	TD02 / TD03
GQ379159	TD02 / TD03
GQ379160	TD02 / TD03
GQ379161	TD02 / TD03
GQ851602	TD02 / TD03
GQ851603	TD02 / TD03
GQ851604	TD02 / TD03
GQ851605	TD02 / TD03
GQ851606	TD02 / TD03
GQ851607	TD02 / TD03
GQ851608	TD02 / TD03
GU011992	TD02 / TD03
GU827998	TD02 / TD03
GU827999	TD02 / TD03
GU828000	TD02 / TD03
GU828001	TD02 / TD03
GU828002	TD02 / TD03
GU828003	TD02 / TD03
GU828004	TD02 / TD03

**Table S4** Summary and comparison of parameter values from Beast analysis, parts A and B

(A) Result of marginal likelihood (log) estimation path sampling and stepping stone sampling methods for West Nile Virus Lineage 2 dataset using different coalescent models, and strict and uncorrelated relaxed log normal molecular clock models. (B) Calculation of best coalescent model and molecular clock model using Bayes factor. Bayes factor range 1-3 means hardly worth mentioning, 3-20 means positive support, 20-150 means strong support and >150 overwhelming support.

Dataset		Sampling	Evolutionary Model			Strict	Uncorrelated relaxed log normal		
<b>Part A</b>	European WNV Lineage 2 complete coding sequences	Stepping stone sampling	Constant			-29244.94581	-29221.69928		
			GMRF SkyRide			-29247.67687	-29221.64373		
			Bayesian SkyGrid			-29245.38443	-29215.06113		
		Path Sampling	Constant			-29248.94892	-29218.79735		
			GMRF SkyRide			-29243.10843	-29216.66507		
			Bayesian SkyGrid			-29242.2842	-29211.11923		

			Strict			Uncorrelated relaxed log normal			
			Constant	GMRF SkyRide	Bayesian SkyGrid	Constant	GMRF SkyRide	Bayesian SkyGrid	
<b>Part B</b>	Stepping stone sampling	Strict	Constant	0.00	-2.73	-0.44	23.25	23.30	29.88
			GMRF SkyRide	2.73	0.00	2.29	25.98	26.03	32.62
			Bayesian SkyGrid	0.44	-2.29	0.00	23.69	23.74	30.32
		Uncorrelated relaxed log normal	Constant	-23.25	-25.98	-23.69	0.00	0.06	6.64
			GMRF SkyRide	-23.30	-26.03	-23.74	-0.06	0.00	6.58
			Bayesian SkyGrid	-29.88	-32.62	-30.32	-6.64	-6.58	0.00
	Path sampling	Strict	Constant	0.00	5.84	6.66	30.15	32.28	37.83
			GMRF SkyRide	-5.84	0.00	0.82	24.31	26.44	31.99
			Bayesian SkyGrid	-6.66	-0.82	0.00	23.49	25.62	31.16
		Uncorrelated relaxed log normal	Constant	-30.15	-24.31	-23.49	0.00	2.13	7.68
			GMRF SkyRide	-32.28	-26.44	-25.62	-2.13	0.00	5.55
			Bayesian SkyGrid	-37.83	-31.99	-31.16	-7.68	-5.55	0.00